918 *Inorg. Chem.* **2011**, *50*, 918–931
DOI: 10.1021/ic101516k

Inorganic Chemistry
Article

Ortho-Hydroxyphenylhydrazo-β-Diketones: Tautomery, Coordination Ability, and Catalytic Activity of Their Copper(II) Complexes toward Oxidation of Cyclohexane and Benzylic Alcohols

Maximilian N. Kopylovich,[†] Kamran T. Mahmudov,[†] M. Fátima C. Guedes da Silva,[†,‡] Paweł J. Figiel,[†] Yauhen Yu. Karabach,[†] Maxim L. Kuznetsov,[†] Konstantin V. Luzyanin,[†] and Armando J. L. Pombeiro*[,†]

[†]*Centro de Química Estrutural, Complexo I, Instituto Superior Técnico, TU Lisbon, Av. Rovisco Pais, 1049-001, Lisbon, Portugal, and* [‡]*Universidade Lusófona de Humanidades e Tecnologias, ULHT Lisbon Av. Campo Grande no. 376, 1749-024, Lisbon, Portugal*

Received July 28, 2010

New hydrazone *o*-HO-phenylhydrazo-β-diketones (OHADB), $R^1NHN{=}CR^2R^3$ [R^1 = HO-2-C_6H_4, R^2 = R^3 = COMe (H_2L^1, **1**), R^2R^3 = $COCH_2C(Me)_2CH_2CO$ (H_2L^2, **2**), R^2 = COMe, R^3 = COOEt (H_2L^4, **4**); R^1 = HO-2-O_2N-4-C_6H_3, R^2R^3 = $COCH_2C(Me)_2CH_2CO$ (H_2L^3, **3**), R^2 = COMe, R^3 = COOEt (H_2L^5, **5**), R^2R^3 = COMe (H_2L^6, **6A**)], and their Cu(II) complexes $[Cu_2(CH_3OH)_2(\mu\text{-}L^1)_2]$ **7**, $[Cu_2(H_2O)_2(\mu\text{-}L^2)_2]$ **8**, $[Cu(H_2O)(L^3)]$ **9**, $[Cu_2(\mu\text{-}L^4)_2]_n$ **10**, $[Cu(H_2O)(L^5)]$ **11**, $[Cu_2(H_2O)_2(\mu\text{-}L^6)_2]$ **12A** and $[Cu(H_2O)_2(L^6)]$ **12B** were synthesized and fully characterized, namely, by X-ray analysis (**4**, **5**, **7**−**12B**). Reaction of **6A**, $Cu(NO_3)_2$ and ethylenediamine (**en**) leads, via Schiff-base condensation, to $[Cu\{H_2NCH_2CH_2N{=}C(Me)C(COMe){=}NNC_6H_3\text{-}2\text{-}O\text{-}4\text{-}NO_2\}]$ (**13**), and reactions of **12A** and **12B** with en give the Schiff-base polymer $[Cu\{H_2NCH_2CH_2N{=}C(Me)C(COMe){=}NNC_6H_3\text{-}2\text{-}O\text{-}4\text{-}NO_2\}]_n$ **14**. The dependence of the OHADB tautomeric equilibria on temperature, electronic properties of functional groups, and solvent polarity was studied. The OHADB from *unsymmetrical* β-diketones exist in solution as a mixture of enol-azo and hydrazo tautomeric forms, while in the solid state all the free and coordinated OHADB crystallize in the hydrazo form. The relative stabilities of various tautomers were studied by density functional theory (DFT). **7**−**14** show catalytic activities for peroxidative oxidation (in $MeCN/H_2O$) of cyclohexane to cyclohexanol and cyclohexanone, for selective aerobic oxidation of benzyl alcohols to benzaldehydes in aq. solution, mediated by TEMPO radical, under mild conditions and for the MW-assisted solvent-free synthesis of ketones from secondary alcohols with *tert*-butylhydroperoxide as oxidant.

Introduction

Azoderivatives of β-diketones (ADB, Scheme 1) represent a class of compounds known for a long time but with a surprisingly low impact in coordination chemistry. It was postulated[1,2] that ADB may exist in three tautomeric forms (enol-azo, keto-azo, and hydrazo; see below) allowing their application for the design of functional materials attributed to smart hydrogen bonding, bistate molecular switches, self-assembled layers, liquid crystals, and so forth.[2] However, experimentally it was found that the studied ADB are stabilized in the hydrazo form with formation of a hydrogen bond between the hydrazone =N−NH− moiety and a carbonyl group giving a six-membered cycle (Scheme 1). In contrast to the well-studied chemistry of β-diketones, the number of publications devoted to ADB coordination compounds is very limited,[3] and the structurally characterized complexes are usually simple diligand monomeric chelates.[3a,c] Thus, to promote the versatility of coordination of ADB, we decided to focus on a functionalized form, in particular the *ortho*-hydroxyphenyl

*To whom correspondence should be addressed. Fax: (+351) 218464455. E-mail: pombeiro@ist.utl.pt.

(1) (a) Pendergrass, J. D. B.; Paul, I. C.; Curtin, D. Y. *J. Am. Chem. Soc.* **1972**, *94*, 8730. (b) Michael, G. B. D.; Brian, V.; Gerald, R. W. *J. Chem. Soc. Perkin Trans. 2* **1982**, 1297. (c) Ide, S.; Kendi, E.; Ertan, N. *J. Chem. Crystallogr.* **1994**, *24*, 743. (d) Marten, J.; Seichter, W.; Weber, E.; Bohme, U. *J. Phys. Org. Chem.* **2007**, *20*, 716. (e) Gawinecki, R.; Kolehmainen, E.; Janota, H.; Kauppinen, R.; Nissinen, M.; Osmialowski, B. *J. Phys. Org. Chem.* **2001**, *14*, 797. (f) Bustos, C.; Sanchez, C.; Martınez, R.; Ugarte, R.; Schott, E.; Mac-Leod, C. D.; Garland, M. T.; Espinoza, L. *Dyes Pigm.* **2007**, *74*, 615. (g) Tayyari, S. F.; Sammelson, R. E.; Tayyari, F.; Rahemi, H.; Ebrahimi, M. *J. Mol. Struct.* **2009**, *920*, 301. (h) Seth, S.; Aravindakshan, K. K. *Synth. React. Inorg., Met.-Org., Nano-Met. Chem.* **2009**, *39*, 345.

(2) (a) Bertolasi, V.; Ferretti, V.; Gilli, P.; Gilli, G.; Issa, Y. M.; Sherif, O. E. *J. Chem. Soc., Perkin Trans. 2* **1993**, 2223. (b) Bertolasi, V.; Gilli, P.; Ferretti, V.; Gilli, G.; Vaughan, K. *New J. Chem.* **1999**, *23*, 1261. (c) Gilli, P.; Bertolasi, V.; Pretto, L.; Lycka, A.; Gilli, G. *J. Am. Chem. Soc.* **2002**, *124*, 13554. (d) Marten, J.; Erbe, A.; Critchley, K.; Bramble, J. P.; Weber, E.; Evans, S. D. *Langmuir* **2008**, *24*, 2479. (e) Jeong, M. J.; Park, J. H.; Lee, C.; Chang, J. Y. *Org. Lett.* **2006**, *8*, 2221.

(3) (a) Marten, J.; Seichter, W.; Weber, E. *Z. Anorg. Allg. Chem.* **2005**, *631*, 869. (b) Mishra, L.; Yadaw, A. K.; Srivastava, S.; Patel, A. B. *New J. Chem.* **2000**, *24*, 505. (c) Weber, E.; Marten, J.; Seichter, W. *J. Coord. Chem.* **2009**, *62*, 3401. (d) Maharramov, A. M.; Aliyeva, R. A.; Mahmudov, K. T.; Kurbanov, A. V.; Askerov, R. K. *Russ. J. Coord. Chem.* **2009**, *35*, 704.

 Published on Web 01/06/2011

Scheme 1. Intramolecular Hydrogen Bonds in ADB and OHADB

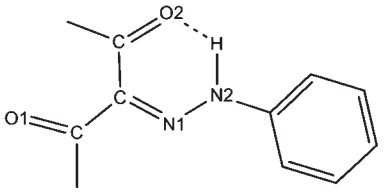

ADB

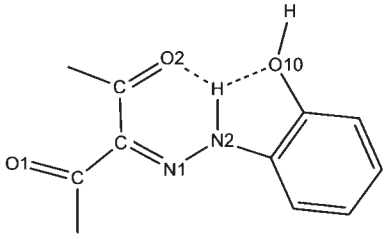

OHADB

substituted ADB (OHADB, Scheme 1), in view of the promising coordination features of these compounds.

In fact, a comparison of our previous observations[4,5] with literature data[6] shows that OHADB drastically differ in physicochemical, analytical, and coordination properties from β-diketones and simple ADB. Relevant differences between OHADB and ADB can be accounted for by the formation, in the former, of one further intramolecular H-bond, whereby the $=N-\underline{N}H$ hydrogen can be shared between the C=O(2) and $-O(10)\overline{H}$ groups (Scheme 1). As a result, a transition of the hydrazo proton to the carbonyl moiety is facilitated and the mole fraction of the enol-azo form, acid properties, and reactivity should increase. This phenomenon is worth to be investigated in detail, in particular to try and find a dependence of the relative amounts of the tautomers (hydrazo and enol-azo, see below) on the OHADB structure, temperature, solvent polarity, and so forth.

In addition, the *ortho*−OH group close to the hydrazone moiety can create one more metal chelating site with a stabilizing effect on the respective complex. This would facilitate the formation of complexes, for example, with Cu(II), hopefully with different primary structures and overall topologies. Thus, another aim is to test the versatility of OHADB to prepare different types of copper(II) complexes by varying the synthetic conditions and by using amines as reagents for Schiff-base template condensations.[7]

Ligand lability can be favorable to catalytic activity, and our preliminary studies have shown that related copper(II) complexes containing labile sites (coordinated water molecules) are significantly active in some oxidation reactions.[4a] Other copper complexes with N,O-ligands display a high catalytic activity in cyclohexane oxidation, for example, some multinuclear Cu compounds that mimic the particulate methane monooxygenase function.[8] On the other hand, the application of TEMPO (2,2,6,6-tetramethylpiperidine-1-oxyl) radical (or its derivatives) with copper complexes for the aerobic oxidation of benzyl alcohols to aldehydes has been studied intensively during the past years, with regard to the selective oxidation of alcohols by dioxygen or air.[9] Hence, the current work also aimed to apply the OHADB-Cu(II) complexes as catalyst precursors for the above types of oxidations.

Thus, having in mind the above-mentioned considerations, the main objectives of the present study are as follows: (i) to synthesize new ADB with an *ortho*−OH group at the aromatic ring (i.e., OHADB), as well as with other substituents; (ii) to study the influence of temperature, solvents, and substituents on the tautomeric equilibria of the obtained OHADB; (iii) to synthesize new complexes of these OHADB with Cu(II) and study the structural influences of substituents and synthetic conditions; (iv) to check the catalytic activity of the synthesized copper(II) complexes in the above-mentioned oxidation reactions.

Results and Discussion

Synthesis of OHADB and Their Structural Properties. 3-(2-Hydroxyphenylhydrazo)pentane-2,4-dione (H_2L^1, **1**), 5,5-dimethyl-2-(2-hydroxyphenylhydrazo)cyclohexane-1, 3-dione (H_2L^2, **2**), 5,5-dimethyl-2-(2-hydroxy-4-nitrophenylhydrazo)cyclohexane-1,3-dione (H_2L^3, **3**), 1-ethoxy-2-(2-hydroxyphenylhydrazo)butane-1,3-dione (H_2L^4, **4**), 1-ethoxy-2-(2-hydroxy-4-nitrophenylhydrazo)butane-1,3-dione (H_2L^5, **5**), and 3-(2-hydroxy-4-nitrophenylhydrazo)-pentane-2,4-dione (H_2L^6, **6A**) (Scheme 2) were synthesized via the Japp−Klingemann reaction[10] between the respective aromatic diazonium salts and β-diketones in an ethanolic

(4) (a) Mahmudov, K. T.; Kopylovich, M. N.; Guedes da Silva, M. F. C.; Figiel, P. J.; Karabach, Y. Yu.; Pombeiro, A. J. L. *J. Mol. Catal. A: Chem.* **2010**, *318*, 44. (b) Aliyeva, R. A.; Pashaev, F. G.; Gasanov, A. G.; Mahmudov, K. T. *Russ. J. Inorg. Chem.* **2009**, *54*, 1407.

(5) (a) Mahmudov, K. T.; Aliyeva, R. A.; Gadjieva, S. R.; Chyragov, F. M. *J. Anal. Chem.* **2008**, *63*, 435. (b) Mahmudov, K. T.; Maharramov, A. M.; Aliyeva, R. A.; Aliyev, I. A.; Kopylovich, M. N.; Pombeiro, A. J. L. *Anal. Lett.* **2010**, *43*, 2923.

(6) (a) Aromi, G.; Gamez, P.; Reedijk, J. *Coord. Chem. Rev.* **2008**, *252*, 964. (b) Vigato, P. A.; Peruzzo, V.; Tamburini, S. *Coord. Chem. Rev.* **2009**, *253*, 1099.

(7) (a) Gimeno, N.; Vilar, R. *Coord. Chem. Rev.* **2006**, *250*, 3161, and references therein. (b) Givaja, G.; Blake, A. J.; Wilson, C.; Schroder, M.; Love, J. B. *Chem. Commun.* **2005**, *35*, 4423. (c) Chattopadhyay, S.; Drew, M. G. B.; Ghosh, A. *Polyhedron* **2007**, *26*, 3513. (d) Aguiari, A.; Brianese, N.; Tamburini, S.; Vigato, P. A. *Inorg. Chim. Acta* **1995**, *235*, 233. (e) Sandi-Urena, S.; Parsons, E. J. *Inorg. Chem.* **1994**, *33*, 302.

(8) (a) Kirillov, A. M.; Kopylovich, M. N.; Kirillova, M. V.; Haukka, M.; Guedes da Silva, M. F. C.; Pombeiro, A. J. L. *Angew. Chem., Int. Ed.* **2005**, *44*, 4345. (b) Karabach, Y. Yu.; Kirillov, A. M.; Haukka, M.; Kopylovich, M. N.; Pombeiro, A. J. L. *J. Inorg. Biochem.* **2008**, *102*, 1190. (c) Contaldi, S.; Di Nicola, C.; Garau, F.; Karabach, Y. Yu.; Martins, L. M. D. R. S.; Monari, M.; Pandolfo, L.; Pettinari, C.; Pombeiro, A. J. L. *Dalton Trans.* **2009**, 4928. (d) Nesterov, D. S.; Kokozay, V. N.; Dyakonenko, V. V.; Shishkin, O. V.; Jezierska, J.; Ozarowski, A.; Kirillov, A. M.; Kopylovich, M. N.; Pombeiro, A. J. L. *Chem. Commun.* **2006**, 4605. (e) Kirillov, A. M.; Karabach, Y. Yu.; Haukka, M.; Guedes da Silva, M. F. C.; Sanchiz, J.; Kopylovich, M. N.; Pombeiro, A. J. L. *Inorg. Chem.* **2008**, *47*, 162. (f) Kirillova, M. V.; Kirillov, A. M.; Pombeiro, A. J. L. *Adv. Synth. Catal.* **2009**, *351*, 2936. (g) Kirillova, M. V.; Kozlov, Y. N.; Shul'pina, L. S.; Lyakin, O. Y.; Kirillov, A. M.; Talsi, E. P.; Pombeiro, A. J. L.; Shul'pin, G. B. *J. Catal.* **2009**, *268*, 26. (h) Shul'pin, G. B.; Kozlov, Y. N.; Nizova, G. V.; Suss-Fink, G.; Stanislas, S.; Kitaygorodskiy, A.; Kulikova, V. S. *J. Chem. Soc., Perkin Trans. 2* **2001**, *2*, 1351.

(9) (a) Vogler, T.; Studer, A. *Synthesis-Stuttgart* **2008**, 1979. (b) Liu, J. H.; Wang, F.; Fu, X. L. *Prog. Chem.* **2007**, *19*, 1718. (c) De Souza, M. V. N. *Mini-Rev. Org. Chem.* **2006**, *3*, 155. (d) Sheldon, R. A. *J. Mol. Catal. A: Chem.* **2006**, *251*, 200. (e) Calderon, F. *Synlett*. **2006**, 657. (f) Sheldon, R. A.; Arends, I. W. C. E. *Adv. Synth. Catal.* **2004**, *346*, 1051. (g) Minisci, F.; Recupero, F.; Pedulli, G. F.; Lucarini, M. *J. Mol. Catal. A: Chem.* **2003**, *63*, 204.

(10) (a) Japp, F. R.; Klingemann, F. *Liebigs Ann. Chem.* **1888**, *247*, 190. (b) Yao, H. C.; Resnick, P. *J. Am. Chem. Soc.* **1962**, *84*, 3514. (c) Yao, H. C. *J. Org. Chem.* **1964**, *29*, 2959.

Scheme 2. *Ortho*-Hydroxy Substituted Azoderivatives of β-Diketones (OHADB) Studied in This Work

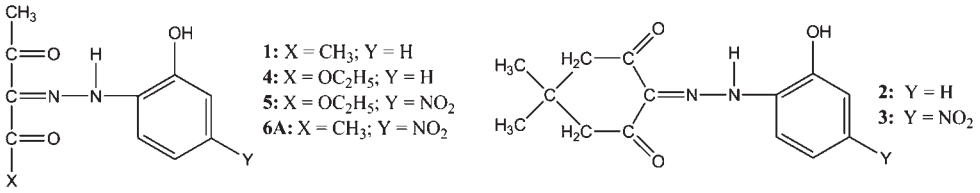

Scheme 3. Possible Tautomeric Transitions of OHADB[a]

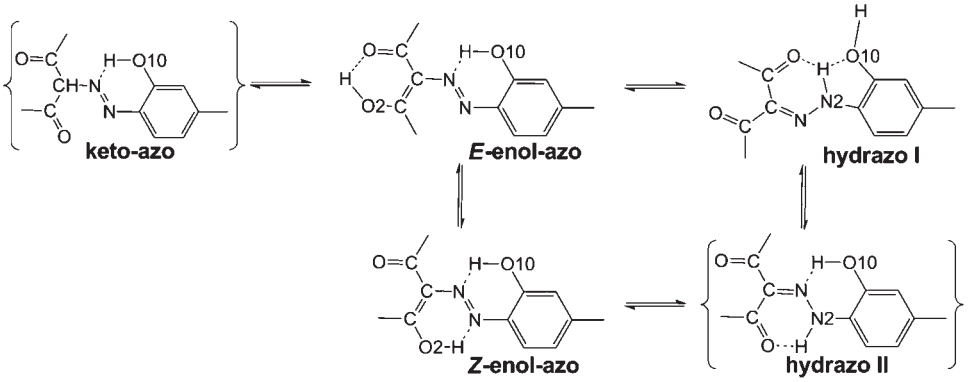

[a] Hypothetical forms which have no experimental support are shown in {} brackets.

solution containing sodium acetate. The compound **6A** was described by us earlier,[4a] and thus will not be discussed in detail now, but will be considered for comparative purposes.

The IR spectra of the OHADB compounds **1**−**6A** (relevant features are provided in the Supporting Information, Table S1) reveal the presence of OH and NH vibrations at about 3180−3468 and 2952−3100 cm^{-1}, correspondingly. The carbonyl stretchings [ν(C═O) 1638−1670, ν(C═O···H) 1616−1632 cm^{-1}] and the ν(C═N) (1569−1601 cm^{-1}) vibrations indicate that, in the solid state, **1**−**6A** are stabilized in the H-bonded hydrazone forms. This is also supported by X-ray and NMR data.

The ^{1}H NMR spectra of the OHADB from *symmetric* β-diketones (**1**−**3**, and **6A**) show only one set of signals for each compound in CD_3OD, CD_3CN or DMSO-d_6. The broad signal at δ about 14−15 is assigned to =N−N<u>H</u> adjacent to the aryl unit. Two methyl groups of the β-diketone moiety yield two resolved singlets, presumably because of the formation of an intramolecular six-membered H-bonded ring (Scheme 3, hydrazo) as it has been reported for the simple ADB.[1−5,10−12] Moreover, the two C═O resonances in the ^{13}C{^{1}H} NMR spectra in the δ 163.8−206.3 range and the single C═N resonance at about 129−137 indicate that **1**−**3** and **6A** exist in solution in the hydrazo form (Scheme 3, Supporting Information, Table S2).

The ^{1}H NMR spectra of the OHADB from *unsymmetrical* β-diketones (**4**, **5**) in DMSO-d_6 at 20−25 °C consist of two sets of signals, indicating they exist in this solvent as a mixture of two tautomeric forms (enol-azo and hydrazo, see below). To identify these forms, and to determine their relative amounts, two-dimensional (2D) correlation and variable temperature NMR experiments in both protic (CD_3OD) and aprotic (CD_3CN) solvents were performed (Supporting Information, Figures S1, S2, Table S2). These data indicate that in both solvents the tautomeric equilibrium exists with comparable amounts of both forms, although dependent on the conditions and the substituents. Thus, with a decrease of temperature and of the electron-withdrawing properties of the substituents, the tautomeric balance shifts to the hydrazo form, while a decrease in solvent polarity increases the mole fraction of

(11) (a) Kitaev, Y. P.; Budnikov, G. K.; Maslova, L. *Izv. Akad. Nauk SSSR Ser. Khim.* **1967**, *9*, 1906. (b) Malik, W.; Goyal, R. N.; Mahest, V. K. *Electroanal. Chem.* **1975**, *62*, 451. (c) Hassib, H. B.; Issa, Y. M.; Mohamed, W. S. *J. Therm. Anal. Calorim.* **2008**, *92*, 775. (d) Garg, H. G.; Sharma, R. A. *J. Med. Chem.* **1969**, *12*, 1122. (e) Garg, H. G.; Sharma, R. A. *J. Med. Chem.* **1970**, *13*, 763. (f) Chen, Z.; Huang, F.; Wu, Y.; Gu, D.; Gan, F. *Inorg. Chem. Commun.* **2006**, *9*, 21. (g) Chen, Z.; Wu, Y.; Gu, D.; Gan, F. *Dyes Pigm.* **2008**, *76*, 624. (h) Shchegol'kov, E. V.; Khudina, O. G.; Anikina, L. V.; Burgart, Y. V.; Saloutin, V. I. *Pharm. Chem. J.* **2006**, *40*, 373. (i) Oruch, E. E.; Kochyigit-Kaymakchoglu, B.; Oral, B.; Altunbas-Toklu, H. Z.; Kabasakal, L.; Rollas, S. *Arch. Pharm. Chem. Life Sci.* **2006**, *339*, 267. (j) Nigam, S. C.; Saharia, G. S.; Sharma, H. R. *Def. Sci. J.* **1982**, *32*, 87. (k) Kuchukguzel, G. S.; Rollas, S.; Kuchukguzel, I.; Kiraz, M. *Eur. J. Med. Chem.* **1999**, *34*, 1093. (l) El Ashry, E. S. H.; Awad, L. F.; Ibrahim, E. I.; Bdeewy, O. K. *Chin. J. Chem.* **2007**, *25*, 570. (m) Sokolnicki, J.; Legendziewicz, J.; Amirkhanov, W.; Ovchinnikov, V.; Macalik, L.; Hanuza, J. *Spectrochim. Acta, Part A.* **1999**, *55*, 349. (n) Huang, F.; Wu, Y.; Gu, D.; Gan, F. *Thin Solid Films* **2005**, *483*, 251.

(12) (a) Attanasi, O. A.; Filippone, P.; Fiorucci, C.; Mantellini, F. *Tetrahedron Lett.* **1999**, *40*, 3891. (b) Khudina, O. G.; Burgart, Y. V.; Murashova, N. V.; Saloutin, V. I. *Russ. Org. Chem.* **2003**, *39*, 1421. (c) Kelin, A. V.; Maioli, A. *Current Org. Chem.* **2003**, *7*, 1855. (d) Shchegol'kov, E. V.; Burgart, Y. V.; Khudina, O. G.; Saloutin, V. I.; Chupakhin, O. N. *Russ. Chem. Bull.* **2004**, *53*, 2584. (e) Simunek, P.; Bertolasi, V.; Peskova, M.; Machacek, V.; Lycka, A. *Org. Biomol. J. Chem.* **2005**, *3*, 1217. (f) Mijin, D.; Uscumlic, G.; Perisic-Janjic, N.; Trkulja, I.; Radetic, M.; Jovancic, P. *J. Serb. Chem. Soc.* **2006**, *71*, 435. (g) Elassar, A-Z. A.; Dib, H. H.; Al-Awadi, N. A.; Elnagdi, M. H. *Arkivoc* **2007**, No. ii, 272. (h) Shchur, I. V.; Khudina, O. G.; Burgart, Y. V.; Saloutin, V. I.; Grishina, M. A.; Potemcin, V. A. *Russ. J. Org. Chem.* **2007**, *43*, 1781. (i) Khudina, O. G.; Shchegol'kov, E. V.; Burgart, Ya. V.; Saloutin, V. I.; Bukhvalov, D. V.; Starichenko, D. V.; Shvachko, Y. N.; Korolev, A. V.; Ustinov, V. V.; Aleksandrov, G. G.; Eremenko, I. L.; Kazheva, O. N.; Shilov, G. V.; Dyachenko, O. A.; Chupakhin, O. N. *Russ. Chem. Bull., Int. Ed.* **2007**, *56*, 108.

Scheme 4. Schematic Representations of Complexes **7**−**11**

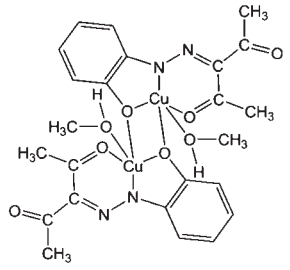

7

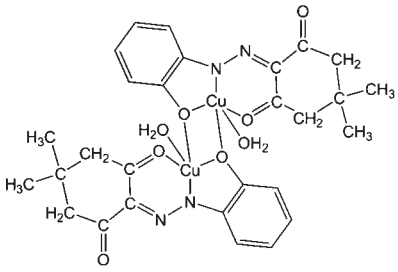

8

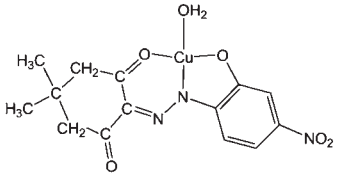

9

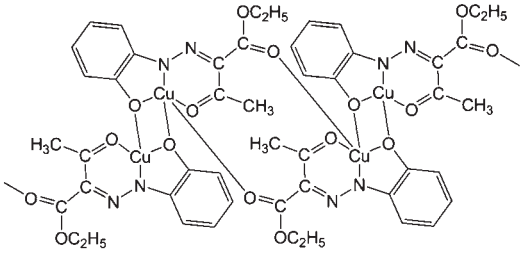

10

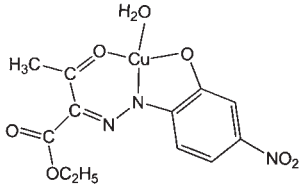

11

the enol-azo form of **5** (the opposite is observed for **4**). Moreover, in the more polar CD_3CN (as compared to CD_3OD), the concentration of the enol-azo tautomer (less polar form) decreases faster with a temperature drop. It should be mentioned that these NMR experiments do not allow to distinguish between the *E*- and *Z*- enol-azo tautomers (Scheme 3). The third tautomeric form, namely, keto-azo, was not detected in solution under any experimental conditions, presumably because of its lower stability in comparison with the others. Gradient enhanced 2D correlation NMR spectra allow to discriminate the carbon signals of the carbonyl groups from the imine moieties for each tautomer (Supporting Information, Figure S2), showing that tautomerization occurs on the side of the molecule that bears the stronger electron-donor ethoxy substituent.[13] Hence, using those data, one can predict and tune the tautomeric equilibrium, and that can be of a particular importance for many applications.[2,5,11]

All the previous studies on the tautomery of ADB describe their existence (both in solution and in solid phase) only in the hydrazo form with formation of the hydrogen bond involving the hydrazone =N−NH− moiety and a carbonyl group forming a six-membered cycle (Scheme 1).[1,2,11,12] It was also shown that the presence of electron-withdrawing and -donating functional groups at the β-diketone fragments and at the aromatic ADB ring influences the O2···N2 distance (Scheme 1) within that hydrogen bonded six-membered cycle,[1d−f,2b,2c] ranging from 2.54 to 2.70 Å, and corresponding, for example, to the following sequence: −COOH (2.587(2)) ≥ −H (2.580(4)) ≥ $-NO_2$ (2.578(1)) > $-CH_3$ (2.562(1)) > −CN (2.541(5)) for substituents in *ortho* position of the aromatic part of ADB. In the case of OHABD, the presence of the *ortho*−OH group must also significantly change the O···N distance because of one more intramolecular H-bond formation between this −OH group and the hydrogen atom of the hydrazone =N−NH− moiety (Scheme 1). This should strengthen the tension on the 6-membered cycle and weaken the N−H bond. The tension rises with the temperature and hence the N−H bond should weaken further and promote the proton transfer to the O2 of the carbonyl moiety. On the other hand, the more asymmetric and longer the groups attached to the carbonyl moieties and to the aromatic part of OHADB are, the more uncompensated would be the movement of the molecule and its amplitude. Hence, the easier should be the tautomeric conversion to the enol-azo form. It should also be mentioned that the *ortho*−OH group of OHADB increases the number of possible isomers (Scheme 3), which can promote the coordination versatility.

To further study the structural features of OHADB and to find out which tautomeric form is stabilized in the solid state, we performed the X-ray analyses of **4** and **5** at 299 (or 295) and 150 K (Supporting Information, Table S2, Scheme S1). The study at different temperatures was performed to find out if the temperature can affect the tautomeric competition with intramolecular proton transfer, as was found by us in solution by NMR (see above) and reported[2c] for the related ketohydrazone-azoenol system in the solid phase. However, all the X-ray structures of

(13) Hansch, C.; Leo, A.; Taft, W. R. *Chem. Rev.* **1991**, *91*, 165.

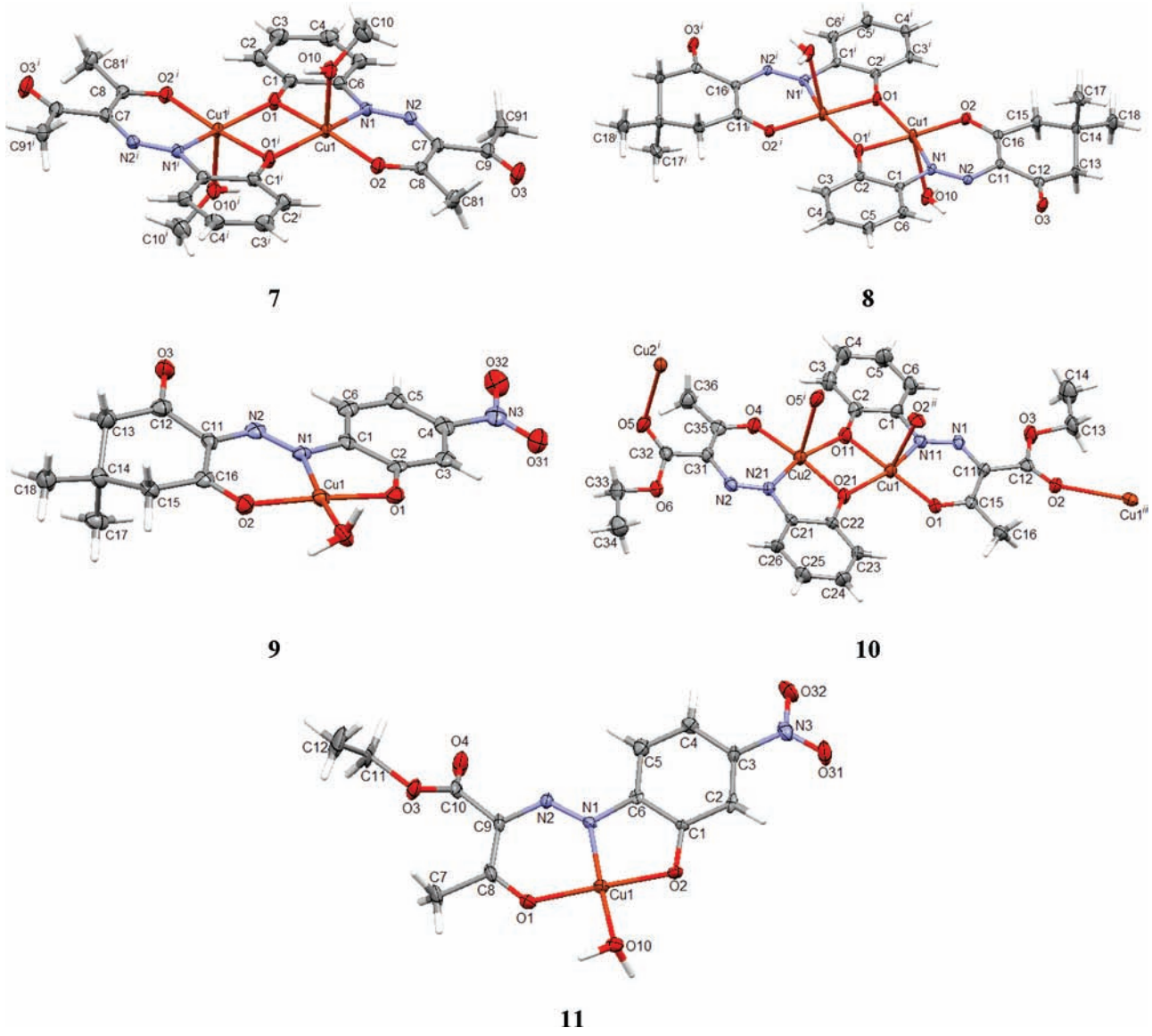

Figure 1. X-ray molecular structures of complexes **7**−**11** with atom numbering schemes. Ellipsoids are drawn at 50% probability. Symmetry operations to generate equivalent atoms: (*i*) $-x, 1-y, 2-z$ (**7**); (*i*) $1-x, -y, 2-z$ (**8**); (*i*) $1/2-x, -1/2-y, -z$ and (*ii*) $1/2-x, -1/2+y, 1/2+z$ (**10**). In **11** only one of the molecules of the asymmetric unit is shown.

the studied compounds show that they crystallize in the hydrazo form I (Supporting Information, Figure S3, Scheme 3).

Therefore, on the basis of IR, NMR, theoretical calculations (See Supporting Information, Tables S3, S4), and X-ray structural analyses, we can conclude that the studied OHADB derived from *symmetric* β-diketones exist in solution and in the solid phase mainly in the hydrazo form, while those derived from *unsymmetric* β-diketones are present as a mixture of hydrazo and enol-azo forms in solution, although in the solid phase the hydrazo form predominates.

Complexation of OHADB to Copper(II). Acetone, methanol, or ethanol solutions of **1**−**6B** (for details see Experimental Section) and an aqueous solution of $Cu(NO_3)_2 \cdot 2.5H_2O$ were mixed, refluxed for a short time, and then left for slow evaporation. X-ray quality crystals of **7**−**12B** were usually formed directly in the reaction mixtures. Molecular representations of the isolated complexes **7**−**11** are shown in Scheme 4 while their molecular structures are depicted in Figure 1, with the most relevant bond distances and angles displayed in Table 1.

$[Cu_2(CH_3OH)_2(\mu\text{-}L^1)_2]$ (**7**) and $[Cu_2(H_2O)_2(\mu\text{-}L^2)_2]$ (**8**) are similar; they crystallize as binuclear species, the former with two methanol and the latter with two water ligands, each on the vertex of the square-pyramidal metal coordination sphere (Scheme 4, Figure 1). The copper atoms, however, are not in the plane defined by the coordinated atoms, being slightly shifted in the direction of the coordinated solvent molecules (0.220 and 0.129 Å in **7** and **8**, respectively). In both structures, only half of the molecule is in the asymmetric unit, the metal is in a general position and the inversion center is in the center of a $Cu(\mu\text{-}O)_2Cu$ core. The β-diketone fragments act as tridentate units by means of the deprotonated aromatic OH group in *ortho* position (O1), which bridge the copper(II) atoms, of one of the nitrogen atoms (N1) and of one oxygen atom (O2) from a carbonyl group. The pentacoordinated Cu(II) atoms belong to three different metallacycles: one

Table 1. Selected Bond Distances (Å) and Angles (deg) for Compounds **7**−**14**

	7	**8**	**9**	**10**	**11**	**12**	**13**	**14**
C−O (*coordinated carbonyl*)	1.275(2)	1.269(3)	1.271(5)	1.244(6)[a]	1.275(5)[a]	1.277(11)[a]		
C−O (*free carbonyl*)	1.224(3)	1.233(3)	1.240(5)		1.21(5)[a]	1.225(12)[a]	1.210(11)	
N−N	1.283(2)	1.279(3)	1.295(5)	1.289(5)[a]	1.30(4)	1.289(11)[a]	1.294(9)	1.308(4)
Cu−N	1.9163(17)	1.923(2)	1.930(3)	1.896(4)[a]	1.91(3)	1.904(8)[a]	1.942(7)[a]	1.906(3)[a]
				Cu(μ-O)$_2$Cu Core				
∠ CuOCu (deg)	101.59(6)	102.90(9)		102.09(14)				
∠ OCuO (deg)	78.41(6)	77.10(9)		78.13(12)				
Cu···Cu (Å)	3.0352(5)	3.0561(7)		3.0178(9)				
longest Cu−O (Å)	1.9694(14)	1.9629(18)		1.958(3)				
shortest Cu−O (Å)	1.9476(14)	1.9449(19)		1.932(3)				
				6-Membered Metallacycle				
∠ O−Cu−N (deg)	91.44(6)	93.85(9)	91.05(14)	92.18(14)[a]	90.6(12)[a]	89.6(3)[a]		
Cu−O (Å)	1.9031(13)	1.8960(19)	1.915(3)	1.896(3)[a]	1.91(3)[a]	1.946(6)[a]		
				5-Membered Metallacycle				
∠ O−Cu−N (deg)	84.55(6)	83.97(8)	85.07(13)	83.95(14)[a]	85.5(12)[a]	85.6(3)[a]	86.2(3)	85.87(13)
Cu−O$_{ortho}$ (Å)	1.9477(16)	1.9449(19)	1.935(3)	1.954(3)[a]	1.92(3)[a]	1.946(6)[a]	1.924(6)	1.942(3)

[a] Average value.

endo ring of the Cu_2O_2 core, which is the central planar ring of the molecule, and two fused six- and five-membered exo metallacycle rings. The Cu−O bond distance in the six-membered ring is generally shorter than that in the five-membered one (Table 1), a fact that, together with the larger O−Cu−N angle in the former, can be justified by the decrease in ring constraint.

Specifically in the structure of **7**, the H10B hydrogen of the coordinated methanol interacts with the π cloud of the Cu1−O2−C8−C7−N2-N1 metallacycle (H-*centroid* 3.191 Å). Intermolecular H-bonds [O10−H10···O3, *d*(D···A) 2.675(2) Å, 129.00°] between the molecules lead to one-dimensional (1D) chains along the crystallographic *b* axis; the cohesion between these layers is obtained by van der Waals H···π interactions involving the methyl hydrogen H91C and the C1 < C6 phenyl ring (C−H··· *centroid*, 3.228 Å, 155.2°). The minimum distance between copper atoms in adjacent layers is of 6.6928(6) Å (Supporting Information, Figure S5). In the structure of **8**, on the other hand, intermolecular H-bonds between the coordinated water molecules and the carbonyl oxygens of two vicinal molecules [Supporting Information, Figure S6: O10−H10A···O3, *d*(D···A) 2.792(3) Å, 159(4)°; O10−H10B···O3, *d*(D···A) 2.858(3) Å, 161(3) °] lead to 1D chains. Additionally, intermolecular π···π interactions are observed between the C1 < C6 phenyl ring and the Cu1−N1−N2−C11−C16−O2 metallacycle; the *centroid*··· *centroid* distance of 3.337 Å indicate a reasonably strong π···π interaction (Supporting Information, Figure S6). In the three-dimensional (3D) packing diagram of **8** the molecules are aligned in two different layers, with a relative angle of 73.43° (measured by the planes defined by the Cu_2O_2 cores). Such alignment leads to a supramolecular network which is distinct from that of **7** (Supporting Information, Figure S7). Because of the bulkiness of the chelating ligands, the minimum intermolecular Cu··· Cu distance in **8** (8.0307 Å) is longer than that in **7** (see above).

In contrast with the previous cases, [Cu(H_2O)(L^3)] (**9**) is mononuclear with a tetracoordinated square-planar metal center (Scheme 4, Figure 1). The inclusion of a nitro group in the aromatic part of the diketone in **9** has no clear effect in bond length and angles, as compared with those of **8**, since the dimensions in the six- and five-membered rings are not so dissimilar in both cases (Table 1). The water ligand in **9** is able to establish intermolecular H-bonds with the coordinated O1 atom of a vicinal molecule and the non-coordinated O3 from another one [O10−H10A···O1, *d*(D···A) 2.698(4) Å, 133.00°; O10−H10B···O3, *d*(D···A) 2.663(5) Å, 167.00°] (Supporting Information, Figure S8). The minimum Cu···Cu distance between two adjacent molecules is as short as 5.081 Å.

The structure of **10**, $[Cu_2(\mu\text{-}L^4)_2]_n$, is polymeric with bimetallic repeating units of the type of those found for **7** and **8**. The interconnection of these units is achieved by means of coordination of both the COOEt carbonyl oxygens which take up the apical positions of the square-pyramid coordination sphere around the copper(II) atoms of two differently oriented bimetallic units. Such a coordination leads to quite dissimilar C_{ester}−O_{ester}−Cu angles [115.6(3) and 155.0(3)°] and to a grid-type network where the Cu(μ-O)$_2$Cu planes in adjacent units make angles of 81.19° (Figure 2). The C−O bond distances of the carbonyl oxygens of the ligand skeleton are considerably different [1.271(5) and 1.217(6) Å] leading to a lower average value [1.244(6) Å] as compared to the previously discussed structures (Table 1).

The asymmetric unit of [Cu(H_2O)(L^5)] (**11**; Scheme 4, Figure 1) comprises two mononuclear square-planar molecules with a relative orientation that makes an angle of 25.35° measured by the planes defined by the corresponding metal coordinated atoms. Bond angles and distances in both molecules are quite similar, but the torsion angles for the C−C−O_{ester}−$C_{carbonyl}$ groups are considerably different (156.49° and 176.93° in the Cu1 and Cu2 molecules, respectively). The most significant H-bonds in this structure (Supporting Information, Figure S10) involve the water ligands of both molecules; in each of them, they interact with the carbonyl oxygen of the ester group in an adjacent molecule and with the aromatic oxygen of another one. The crystal structure is further stabilized by medium intense π···π interactions between the aromatic

ring and the six-membered ring of the Cu2 and Cu1 molecules, respectively (*centroid*···*centroid* distances of 3.475 Å). This feature agrees with theoretical calculations of the model $[Cu(H_2O)(L^{5\prime})]$ **11′** with the methoxy group instead of the ethoxy (Supporting Information, Scheme S2) which indicate a strong delocalization of electron density in the six-membered metallacycle.

It was demonstrated[10c] that the six-membered H-bonded cycle (Scheme 1) in unsymmetrical ADB usually involves the carbonyl group of the moiety with the stronger electron-donor group. That is also confirmed in this work for H_2L^4 and H_2L^5; in both cases the hydrazo hydrogen is bonded to the ethoxycarbonyl group of the diketone moiety (Supporting Information, Scheme S1, S2, Figure S3). However, in the corresponding complexes **10** and **11** (Scheme 4, Figure 1) the carbonyl adjunct to the ethoxy group is either free (in **10**) or coordinated to Cu^{II} of another unit, meaning that coordination to copper(II) does not proceed by a simple direct attack of Cu^{II} to the H-bonded C=O···HN···OH moiety. A more complicated mechanism should be considered, conceivably via an initial attack of Cu^{II} to a carbonyl oxygen not involved in H-bond, followed by rupture of H-bonds and ligand deprotonation.

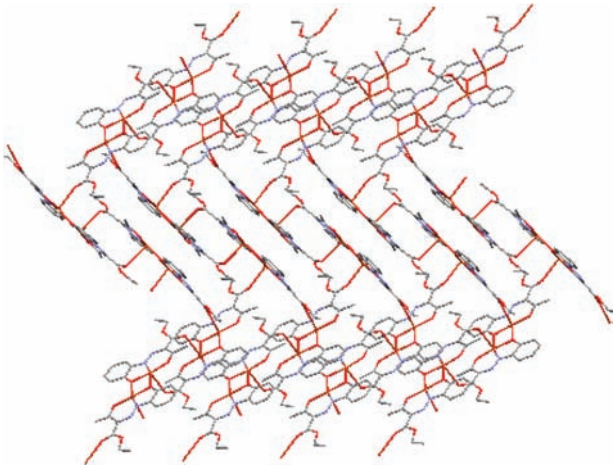

Figure 2. 3D packing diagram of compound **10** (arbitrary view). The grid-type network is achieved by means of dissimilar $C_{ester}-O_{ester}-Cu$ angles. The $Cu(\mu\text{-}O)_2Cu$ planes in adjacent units make angles of 81.19°.

Condensation Reaction of an OHADB Ligand. Complexes of the above type can be used for further and ready synthesis of Schiff-base species, and the viability of this approach is illustrated for the case of H_2L^6 (**6A**). In fact, although free **6A** does not undergo condensation with an amine, for example, ethylenediamine (en), such a reaction readily occurs upon coordination to Cu^{II}, as shown below. Hence, free **6A** is simply deprotonated by en to give the $(H_2en)L^6$ salt (**6B**) (Scheme 5, Route I). The reaction of **6B** with $Cu(NO_3)_2$ hydrate in methanol/water affords the mononuclear complex $[Cu(H_2O)_2(\mu\text{-}L^6)]$ **12B** (Route II) which converts easily into the dinuclear $[Cu_2(H_2O)_2(\mu\text{-}L^6)_2]$ **12A** by simple refluxing a methanol solution of the former (Scheme 5, Route III). **12A** can be also formed in a direct way from reaction of H_2L^6 (**6A**) with $Cu(NO_3)_2$ hydrate (Route IV).[4a]

The X-ray diffraction analysis of $[Cu(H_2O)_2(\mu\text{-}L^6)]$ (**12B**) confirms that copper(II) is pentacoordinated with one water ligand in an equatorial position and the other one in the apical position of a square-pyramid geometry (Supporting Information, Figure S10a). The bond distances and angles are in agreement with the previously discussed structures (see above and Table 1) but, similarly to what was found in **11**, the torsion angles for the $C-C-C_{carbonyl}-C$ ketone groups are different (173.13° and 167.34° in the Cu1 and Cu2 molecules, respectively). The asymmetric unit of **12B**, like that of **11**, also comprises two molecules; nevertheless, the angle of the planes defined by the square environment of each Cu(II) ion is only of 8.43°.

Scheme 5. Other Reactions of Copper(II) with **6A** and Its Modified Form **6B**

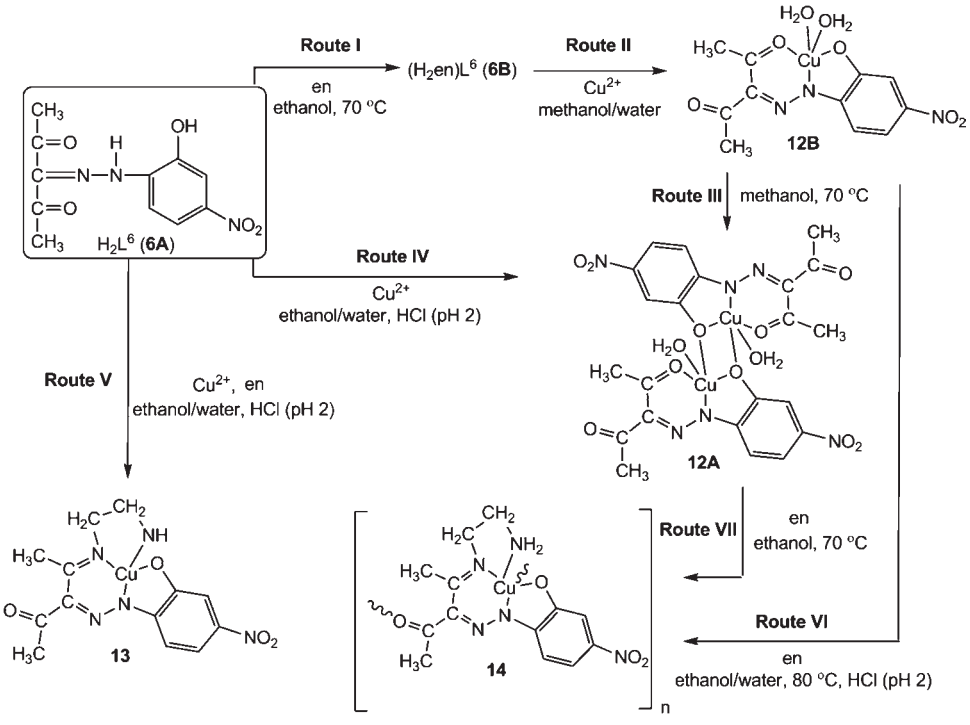

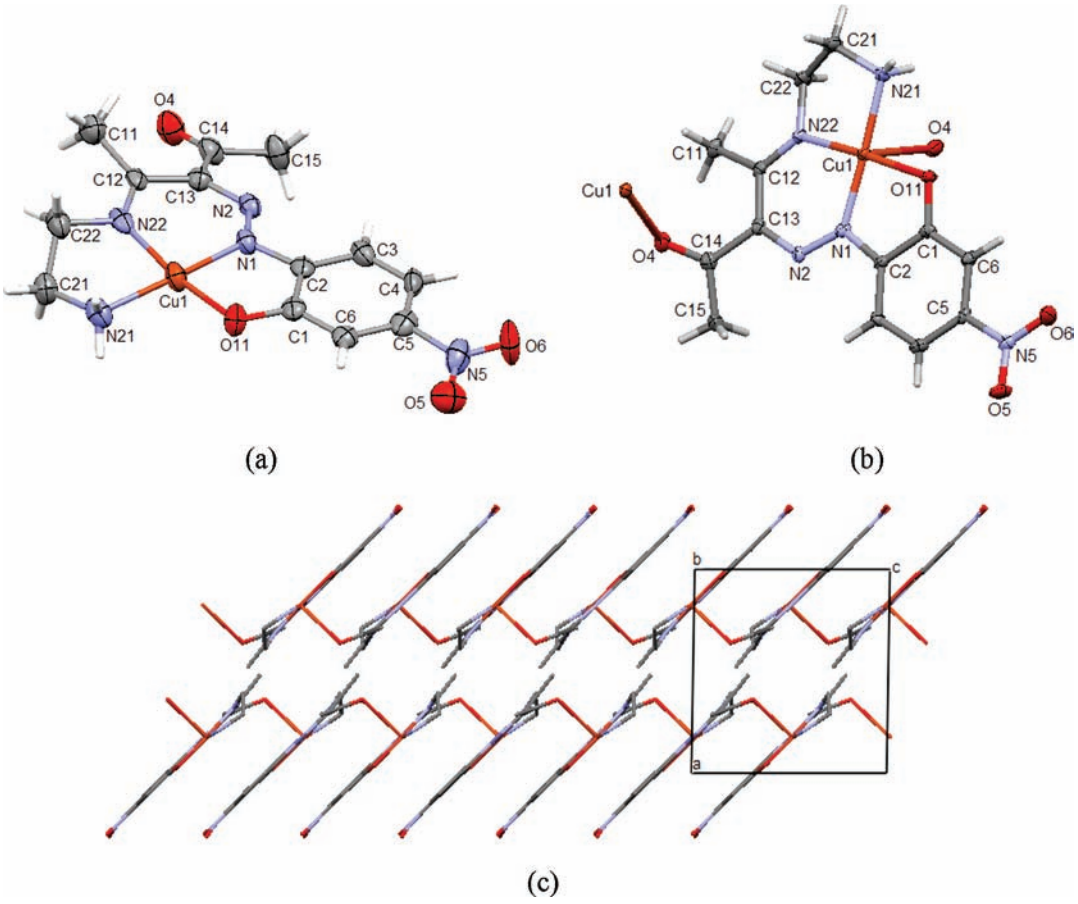

Figure 3. X-ray molecular structures of complexes **13** (a) and **14** (b) with atom numbering scheme and packing diagram of **14** showing a fragment of two 1D chains viewed along the crystallographic *b* axis (c).

Moreover, it is interesting to compare the relative orientation of the molecules in the asymmetric units of both structures: in **11**, one molecule is rotated about 180° in the horizontal plane relative to the other one, but in **12B** the 180° horizontal rotation is associated with a reflection also in the horizontal plane (Supporting Information, Figure S10b). Consequently, the equatorial water molecules in both molecules of **12B** are oriented in the same direction, while in **11** they are pointing to opposite sides. Another relevant feature of **12B** is the $\pi\cdots\pi$ interaction involving the five-membered metallacycle rings with a short *centroid*$\cdots$*centroid* distance of 3.168 Å. Both intra- and intermolecular H-bond interactions were found for **12B**, the former involving methylic hydrogens and N2 (in the Cu1 molecule) or the carbonyl O24 (in the Cu2 molecule) [C15−H15B$\cdots$N2, *d*(D$\cdots$A) 2.684(16) Å, 103.00°; O31−H31B$\cdots$O24, *d*(D$\cdots$A) 2.770(14) Å, 102.00°].

In the presence of $Cu(NO_3)_2$ hydrate, condensation of en with one C=O group of **6A** readily occurs at pH 2 to give the Schiff base complex [Cu{$H_2NCH_2CH_2N$=C(CH_3)C-(C(=O)CH_3)=NNC_6H_3-2-O-4-NO_2}] **13** (Route V). The pH value of 2 is crucial, since for other pH values this metal-promoted (namely, by template effect)[7] reaction does not proceed.

The molecular structure of **13** (Figure 3a) reveals a distorted square planar geometry around the copper(II) ion and confirms its N_3O environment. The C12−N22, C13−N2 and C14−O4 bond lengths of 1.292(11), 1.319(11), and 1.210(11) Å, respectively, indicate double bond characters and a π-electron distribution within the β-diketone fragment. Several intermolecular hydrogen bonds were found in the structure, mainly involving the N21 as H donor, and O4 and O11 as acceptors (Supporting Information, Figure S11). Moreover, reasonably strong H$\cdots\pi$ interactions were located involving the methyl groups of the six-membered metallacycles and the phenyl rings of neighboring molecules (C11−H11$\cdots$*centroid* of 3.171 Å). Such contacts result from the relative positions of the molecules of **13** in space since their planes (defined by the atoms in the coordination sphere of the metal) make angles of 87.84° leading to a 3D grid-type network.

Interestingly, reactions of **12A** and **12B** with en (Routes VI and VII, respectively) provide a coordination polymer, **14** (Figure 3b), with the repeating unit that is a Schiff base complex very similar to **13** (it also bears one six- and two five-membered metallacycles). The Cu1 atom has a square-pyramidal coordination sphere with the tetradentate N_3O ligand occupying the equatorial positions and the apical site being engaged with the O4 atom of the carbonyl group from an adjacent molecule. Although O4 is coordinated to copper, the C14−O4 double bond distance (1.220(5) Å) is not significantly longer than that in **13** (1.210(11) Å). However, the carbonyl O4 atom of each unit is 1.038 Å away from the plane of the molecule (defined by the atoms in the coordination sphere of the metal) and the group is considerably twisted (N2−C13−C14−O4 torsion angle of 155.64°), as compared with **13** (0.880 Å and 174.15°,

Scheme 6. Oxidations of Cyclohexane and Benzyl Alcohol Using OHADB-Cu Complexes As Catalysts

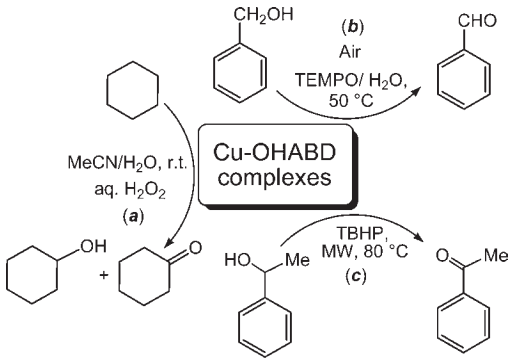

respectively). The 1D coordination polymer thus formed spreads along the crystallographic *c* axis (Figure 3c) in ladder type chains, extending to the second dimension by means of intermolecular hydrogen bonds. The structure is further stabilized by means of $\pi\cdots\pi$ interactions involving the phenyl and the six-membered metallacycle rings of successive steps of the ladder, with *centroid*$\cdots$*centroid* distances of 3.404 Å.

Catalytic Activity of OHADB-Copper(II) Complexes. The oxidations of cyclohexane and benzyl alcohol (Scheme 6) were chosen as model reactions to test the catalytic potential of the synthesized copper compounds **7**−**14** for oxidations of alkanes and alcohols, respectively.

The complexes exhibit good catalytic activities in the peroxidative oxidation of cyclohexane by aqueous H_2O_2, under mild conditions (at 25 °C), to afford cyclohexanol (CyOH) and cyclohexanone (Scheme 6a, Table 2). The total yield, in a single batch, reaches 16−25% (entries 1−6 and 12−14) for the substrate to catalyst molar ratio of 100, whereas turnover number (TON) values up to 60 (entry 8) are reached for the substrate to catalyst molar ratio of 5000. The activities of the mononuclear complexes **9** and **11**, bearing the copper atom with a square planar coordination mode and one ligated water, are similar under standard conditions (product yields lie in 17−19% range, entries 4 and 6). The mononuclear complexes **12B** (which contains copper with a square pyramidal coordination and two ligated water molecules) and **13** (with a distorted square planar geometry) exhibit a slightly higher activity (overall yield of 22−23%, entries 12 and 13). The catalytic activities of the dinuclear complexes **7** and **8** are different (25 and 16% correspondingly, entries 1−3). Such differences possibly reflect the different chelating ligand properties and labilities of the coordinated methanol and water. The reactions performed under higher substrate to catalyst molar ratios (5000) and increased reaction time (24 h) showed similar activities of the dinuclear Cu(II) complexes **7** and **8** (TONs of 55 and 60), and, although smaller, of the mononuclear complexes **9** and **11** (TONs of 35 and 40) (entries 7, 8 and 9, 11, respectively). The polymeric compound **10** exhibits the lowest catalytic activity in the series, what possibly is related to the absence of labile ligands. Generally, the complexes bearing ligands derived from pentane-2,4-dione (**7**, **12B**, **13**) are more active than the others. The reactions performed in the presence of **7** with a low oxidant loading (H_2O_2/cyclohexane molar ratio of 2) and at a higher temperature (50 °C) lead in 1 h to the overall yields of about 17 and 18% under conventional heating or microwave irradiation, correspondingly (entries 15−17).

For the establishment of the mechanism type, experiments in the presence of carbon and oxygen radical traps (TEMPO and diphenylamine, respectively) were performed. Consequently, the addition of TEMPO or Ph_2NH in a stoichiometric amount relative to cyclohexane leads to a marked inhibition of the products formation (compare entries 19 and 20 with 1), signifying that the peroxidative oxidation of cyclohexane proceeds mainly via a radical pathway. Apparently, an hydroxyl radical ($HO^\bullet$) which can be derived from the reduction of hydrogen peroxide by Cu^I (the latter being formed upon oxidation of H_2O_2 to $HOO^\bullet$ by Cu^{II}) abstracts a hydrogen atom from cyclohexane providing the formation of cyclohexyl radical ($Cy^\bullet$), which reacts with O_2 dissolved in the reaction mixture to form cyclohexylperoxyl radical ($CyOO^\bullet$).[8g,h] The latter can undergo either a dismutation (giving ultimately cyclohexanol, cyclohexanone, and dioxygen) or a reduction by Cu^I to the corresponding anion that can be protonated to cyclohexyl hydroperoxide (CyOOH). This can also be formed by H-abstraction of $CyOO^\bullet$ from H_2O_2, and can further undergo metal-assisted decomposition to yield $CyOO^\bullet$ or the alkoxyl radical ($RO^\bullet$) which abstracts hydrogen from cyclohexane forming $Cy^\bullet$ and cyclohexanol.[8,14−18]

The involvment of CyOOH in the formation of the alcohol and ketone is proved by the following observations. At the end of reaction, CyOOH is also present, apart from the alcohol and ketone. However, it is not stable and decomposes at the high temperature of the GC injector/column to the corresponding alcohol and ketone which are the detected products. Following the reported method established by Shul'pin,[17,18] we estimated the amount of CyOOH at the end of the reaction by performing the GC analyses without and with addition of triphenylphosphine, which quantitavely converts CyOOH into CyOH (with formation of $OPPh_3$) (compare entries 1 and 2). CyOOH is thus shown to be the major product at the end of the reaction (ca. 15% yield), while the alcohol and ketone are present in lower amounts (ca. 1 and 9% yields, respectively).

Since $[Cu_2(H_2O)_2(\mu\text{-}L^6)_2]$ (**12A**)[4a] and other copper(II) complexes with N,O-ligands[19] proved to be good catalysts for the aerobic oxidation of benzyl alcohols mediated by TEMPO in aqueous media, we have now applied

(14) Kirillov, A. M.; Kopylovich, M. N.; Kirillova, M. V.; Karabach, Y. Yu.; Haukka, M.; Guedes da Silva, M. F. C.; Pombeiro, A. J. L. *Adv. Synth. Catal.* **2006**, *348*, 159.

(15) (a) Costas, M.; Mehn, M. P.; Jensen, M. P.; Que, L., Jr. *Chem. Rev.* **2004**, *104*, 939. (b) Costas, M.; Chen, K.; Que, L., Jr. *Coord. Chem. Rev.* **2000**, *200*−*202*, 517. (c) Roelfes, G.; Lubben, M.; Hage, R.; Que, L., Jr.; Feringa, B. L. *Chem.*—*Eur. J.* **2000**, *6*, 2152.

(16) Hogan, T.; Sen, A. *J. Am. Chem. Soc.* **1997**, *119*, 2642.

(17) (a) Shul'pin, G. B. *J. Mol. Catal. A: Chem.* **2002**, *189*, 39. (b) Shul'pin, G. B. In *Transition Metals for Organic Synthesis*, 2nd ed.; Beller, M., Bolm, C., Eds.; Wiley-VCH: New York, 2004; Vol. *2*. (c) Shul'pin, G. B. *Organic Reactions Catalyzed by Metal Complexes*; Nauka: Moscow, 1988.

(18) (a) Nizova, G. V.; Krebs, B.; Suss-Fink, G.; Schindler, S.; Westerheide, L.; Cuervo, L. G.; Shul'pin, G. B. *Tetrahedron* **2002**, *58*, 9231. (b) Suss- Fink, G.; Gonzalez, L.; Shul'pin, G. B. *Appl. Catal. A: Gen.* **2001**, *217*, 111. (c) Shul'pin, G. B.; Suss-Fink, G. *J. Chem. Soc., Perkin Trans. 2* **1995**, *2*, 1459. (d) Kodera, M.; Shimakoshi, H.; Kano, K. *Chem. Commun.* **1996**, 1737. (e) Shul'pin, G. B. *C. R. Chim.* **2003**, *6*, 163.

(19) Figiel, P. J.; Kirillov, A. M.; Karabach, Y. Yu.; Kopylovich, M. N.; Pombeiro, A. J. L. *J. Mol. Catal. A: Chem.* **2009**, *305*, 178.

Table 2. Peroxidative Oxidation of Cyclohexane to Cyclohexanol and Cyclohexanone[a]

					yield[b] of products, %				
entry	catalyst	$n(C_6H_{12})/n(Cat.)$	$n(H_2O_2)/n(C_6H_{12})$	reaction time, h	Alc.	Ket.	total[c]	A/K[d]	TON[e]
1	**7**	100	10	6	7.1	16.6	23.7	0.4	23.7
2[f]	**7**	100	10	6	15.1	9.7	24.8	1.6	24.8
3	**8**	100	10	6	5.3	10.3	15.6	0.5	15.6
4	**9**	100	10	6	6.9	12.0	18.9	0.6	18.9
5	**10**	100	10	6	5.9	10.0	15.9	0.6	15.9
6	**11**	100	10	6	5.4	11.7	17.1	0.5	17.1
7	**7**	5000	2	24	0.5	0.6	1.1	0.8	55
8	**8**	5000	2	24	0.6	0.6	1.2	1.0	60
9	**9**	5000	2	24	0.3	0.4	0.7	0.8	35
10	**10**	5000	2	24	0.2	0.3	0.5	0.7	25
11	**11**	5000	2	24	0.3	0.5	0.8	0.6	40
12	**12B**	100	10	6	9.6	13.9	23.4	0.7	23.4
13	**13**	100	10	6	10.0	12.3	22.3	0.8	22.3
14	**12A**	100	10	6	6.0	10.2	16.2	0.6	16.2
15[g,h]	**7**	100	2	1	7.6	9.1	16.7	0.8	16.6
16[g,i]	**7**	100	2	1	11.1	7.1	18.2	1.6	18.2
17[j,i]	**7**	100	2	1	8.2	8.8	17.0	0.9	17.0
18[g,h]	$Cu(NO_3)_2$	100	2	1	2.7	6.4	9.1	0.4	9.1
19[k]	**7**	100	10	6	2.6	3.4	6.0	0.8	6.0
20[l]	**7**	100	10	6	2.5	7.0	9.5	0.4	9.5

[a] Selected data; reaction conditions (unless stated otherwise): C_6H_{12} (1 mmol for entries 1−6, 12−20 and 5 mmol for entries 7−11), MeCN 4 mL, catalyst precursor (0.01 mmol for entries 1−6, 12−20 and 0.001 mmol for entries 7−11), $n(HNO_3)/n(Cat) = 10$, H_2O_2 (10 mmol added as an aqueous 30% solution), 25 °C. [b] Moles of product/100 mols of C_6H_{12}. [c] Cyclohexanol + cyclohexanone. [d] Alcohol (cyclohexanol)/ketone (cyclohexanone) molar ratio. [e] Overall TON values (moles of products/mol of catalyst). [f] GC analysis performed upon addition of PPh_3. [g] In sealed tube under microwave irradiation (10W, 50 °C), H_2O_2 (2 mmol, aqueous 30% solution). [h] 1 mL MeCN. [i] 0.5 mL MeCN. [j] In sealed tube with conventional heating at 50 °C, H_2O_2 (2 mmol, aqueous 30% solution). [k] In the presence of TEMPO (1 mmol). [l] In the presence of diphenylamine (1 mmol).

Table 3. Aerobic Oxidation of Benzyl Alcohols to the Corresponding Benzaldehydes[a]

entry	catalyst	substrate	product	time, h	yield,[b] %
1	**9**	benzyl alcohol	benzaldehyde	6	22
2	**9**	benzyl alcohol	benzaldehyde	22	99
3	**11**	benzyl alcohol	benzaldehyde	22	72
4	**8**	benzyl alcohol	benzaldehyde	22	52
5	**10**	benzyl alcohol	benzaldehyde	22	35
6	**7**	benzyl alcohol	benzaldehyde	22	63
7	**12B**	benzyl alcohol	benzaldehyde	22	79
8	**12A**	benzyl alcohol	benzaldehyde	22	99
9	**13**	benzyl alcohol	benzaldehyde	22	65
10	**9**	4-Me-benzyl alcohol	4-Me-benzaldehyde	22	48
11	**9**	4-Cl-benzyl alcohol	4-Cl-benzaldehyde	22	67
12	**9**	2-Cl-benzyl alcohol	2-Cl-benzaldehyde	22	81
13	**9**	cinnamyl alcohol	cinnamaldehyde	22	62
14	**9**	1-phenylethanol	acetophenone	22	50

[a] Conditions: substrate (3 mmol), catalyst (0.03 mmol (1 mol %)), TEMPO (0.15 mmol (5 mol %)) in aqueous solution of K_2CO_3 (10 mL, 0.1M), 50 °C, 1 atm, air. [b] Moles of product/100 mols of substrate.

the other synthesized copper(II) complexes **7**−**13** to this reaction (Scheme 6b, Table 3). Oxidation of benzyl alcohol (3 mmol) in alkaline (0.1 M K_2CO_3) aqueous solution, in the presence of a catalytic amount of the monomeric complex **9** (0.03 mmol, 1 mol % vs substrate) and TEMPO (0.15 mmol, 5 mol % vs substrate) results in 22% of benzaldehyde yield after 6 h of reaction (entry 1). Prolonging the reaction time to 22 h led to a nearly quantitative yield of benzaldehyde (99%, entry 2). Unexpectedly, among all the tested complexes, the most efficient ones are those with the strong electron-withdrawing nitro group at the phenyl ring (complexes **9**, **11**, **12B**, and **12A**, entries 2, 3, 7 and 8). The other tested complexes (**7**, **8**, and **10**) shown moderate activities (entries 4−6).

Substituted benzyl alcohols can also be converted to the corresponding aldehydes, as known for other systems,[20] with moderate to good yields (entries 10−12). Allylic alcohol (cinnamyl alcohol, entry 13) is also oxidized to cinnamaldehyde in good yield. The oxidation of a secondary benzyl alcohol (1-phenylethanol, entry 14) leads to the corresponding ketone in moderate yield. The limitation of the current system, as usually observed for other catalysts,[21] concerns the failure of application to aliphatic alcohols (results not included in Table 3). As proposed earlier,[21c] Cu/TEMPO catalytic systems follow a mechanism similar to that of the galactose-oxidase enzymes,

(20) (a) Sheldon, R. A. *J. Mol. Catal. A: Chem.* **2006**, *251*, 200. (b) Sheldon, R. A.; Arends, I. W. C. E. *Adv. Synth. Catal.* **2004**, *346*, 1051. (c) Minisci, J. *Mol. Catal. A: Chem.* **2003**, *204*−*205*, 63.

(21) (a) Gamez, P.; Arends, I. W. C. E.; Reedijk, J.; Sheldon, R. A. *Chem. Commun.* **2003**, 2414. (b) Punniyamurthy, T.; Rout, L. *Coord. Chem. Rev.* **2008**, *252*, 134. (c) Lin, L.; Liuyan, J.; Yunyang, W. *Catal. Commun.* **2008**, *9*, 1379. (d) Palombi, L.; Bonadies, F.; Scetti, A. *Tetrahedron* **1997**, *53*, 15867. (e) Figiel, P. J.; Kopylovich, M. N.; Lasri, J.; Guedes da Silva, M. F. C.; Silva, J. J. R. F.; Pombeiro, A. J. L. *Chem. Commun.* **2010**, *46*, 2766.

Table 4. MW-Assisted Oxidation of Benzyl Alcohol and 1-Phenylethanol with TBHP to the Corresponding Carbonyl Compounds with Complex **9** as Catalyst[a]

entry	substrate	product	temp., °C	time, min	yield,[b] %	TON,[c] (TOF)[d]
1	benzyl alcohol	benzaldehyde	50	60	20.1	101
2	1-phenylethanol	acetophenone	80	15	26.1	131 (523)
3	1-phenylethanol	acetophenone	80	30	39.0	195 (390)
4	1-phenylethanol	acetophenone	80	60	82.7	414 (414)
5	1-phenylethanol	acetophenone	80	120	89.0	445 (223)

[a] Conditions: substrate (5 mmol), catalyst (0.01 mmol, 0.2 mol %), TBHP (10 mmol), 50 °C (benzyl alcohol) or 80 °C (1-phenylethanol), 10W. [b] Moles of product/100 mols of substrate. [c] Overall TON values (moles of products/mol of catalyst). [d] TOF = TON/h (values in brackets).

involving coordination of the alcohol and TEMPO to the copper center, and hydrogen abstraction from the alcohol α-carbon by TEMPO. As a result, the formation of TEMPOH and of a subsequent alkoxy-Cu(II) complex is postulated. The latter reacts with another molecule of TEMPO, leading to the aldehyde and TEMPOH, with regeneration of the copper catalyst.

The synthesized complexes were also tested as catalyst precursors for the solvent-free low power (10 W) microwave-assited (MW) peroxidative oxidation[21d,e] of benzyl alcohol and 1-phenylethanol with *tert*-butylhydroperoxide (TBHP) to benzaldehyde and acetophenone, respectively (Scheme 6c, Table 4). Complex **9** showed the highest activity, for example, leading to a benzaldehyde yield of about 20% in 1 h (entry 1), while the use of the other catalyst precursors resulted in about 15% average yield. Thus, **9** was chosen for the studies of the MW-assisted oxidation of 1-phenylethanol, which proceeds more efficiently (acetophenone yields of ca. 83 or 89% were achieved in 1 or 2 h, entries 4 or 5, respectively). Despite the good catalytic activity of the studied complexes, they are less active than some copper(II) triazapentadiene compounds we have previously reported.[21e]

Conclusions

A series of new OHADB were synthesized and fully characterized. The *symmetric* ones are stabilized in solution in the hydrazo form, as known for other ADB, but, for the first time, it was found that the *unsymmetric* OHADB exist in solution in enol-azo and hydrazo forms, though the tautomeric balance is dependent on the solvent polarity and on the electron-withdrawing properties of the substituents at the aromatic ring. These results can help to tune the tautomeric balance to the desired form for different types of applications or further syntheses. X-ray structural analyses show that OHADB exist in the solid state in the hydrazo form with the H−N proton forming hydrogen bonds between one C=O of the β-diketone fragment and the *ortho*-OH group of the aromatic part of the molecule, and that intramolecular hydrogen bonded rings are formed at the side bearing the stronger electron-withdrawing substituents.

Upon complexation with copper(II), the studied OHADB lead to structurally different mono-, bi-, and polynuclear complexes; also a Schiff base template synthesis was performed showing the possibility to form new versatile imino derivatives. OHADB behave as promising ligands toward complexes of different nuclearities forming extended 1D or 2D assemblies via H-bonding or $\pi\cdots\pi$ interactions involving, for example, metallacycle rings.

The complexes act as efficient and selective catalysts for the mild peroxidative oxidation of cyclohexane to the corresponding alcohol and ketone, for the aerobic oxidation (mediated by TEMPO), in aqueous medium, of benzyl alcohols to the corresponding benzaldehydes (up to 99% yield), or for the solvent-free microwave-assisted oxidation of benzyl alcohol and 1-phenylethanol to the corresponding carbonyl products.

Experimental Section

Materials and Instrumentation. All the synthetic work was performed in air and at room temperature. All the chemicals were obtained from commercial sources (Aldrich) and used as received. Infrared spectra (4000−400 cm^{-1}) were recorded on a BIO-RAD FTS 3000MX instrument in KBr pellets. 1D (^1H, $^{13}C\{^1H\}$) and 2D ($^1H,^1H$−COSY, $^1H,^{13}C$-HMQC, $^1H,^{13}C$-HSQC and $^1H,^{13}C$-HMBC) NMR spectra were recorded on Bruker Advance II+ 300.13 (75.468 carbon-13) and 400.13 (100.61 carbon-13) MHz (UltraShield Magnet) spectrometers at ambient temperature. C, H, and N elemental analyses were carried out by the Microanalytical Service of the Instituto Superior Técnico. Electrospray mass spectra were run with an ion-trap instrument (Varian 500-MS LC Ion Trap Mass Spectrometer) equipped with an electrospray (ESI) ion source. For electrospray ionization, the drying gas and flow rate were optimized according to the particular sample with 35 psi nebulizer pressure. Scanning was performed from m/z 100 to 1200 in methanol solution. The compounds were observed in the positive mode (capillary voltage = 80−105 V). Chromatographic analyses were undertaken by using a Fisons Instruments GC 8000 series gas chromatograph with a DB-624 (J&W) capillary column (FID detector) and the Jasco-Borwin v.1.50 software.

Synthesis of the *ortho*-Hydroxy Substituted Phenylhydrazo-β-diketones (OHADB). These compounds were prepared via the Japp−Klingemann reaction involving diazotization of aromatic amines with following azocoupling of the thus formed diazonium salt and a dione.[10]

Diazotization. A 0.025 mol portion of an *ortho*-aminophenol was dissolved in 50 mL of water upon addition of 1.0 g of crystalline NaOH. The solution was cooled in an ice bath to 0 °C and 1.725 g, 0.025 mol of $NaNO_2$ was added with subsequent addition of 5 mL 33% HCl in portions of 0.2 mL for 1 h under rigorous stirring. During the reaction the temperature of the mixture must not exceed +5 °C. A suspension of the unstable 2-hydroxyphenyldiazonium chloride was obtained which was then used as such for the next stage (see below).

Azocoupling. A 5.0 g portion of CH_3COONa was added to a mixture of 0.025 mol of β-diketones with 50 mL of ethanol. The solution was cooled in an ice bath, and a suspension of the *ortho*-aminophenol diazonium salt (prepared according to the procedure described above) was added in two equal portions under vigorous stirring for 1 h. Along this stage, the pH must be maintained in the range of 8−10; crystalline CH_3COONa may be added if needed. On the next day, the formed precipitate of the ligand was filtered off, washed with water, recrystallized from ethanol, and dried in air. The characterizations of the ligands were carried out by IR, element analysis, ^1H and ^{13}C NMR spectroscopies and are given below.

Compound 1. Yield: 72% (based on pentane-2,4-dione), black powder soluble in methanol, ethanol, acetone and insoluble in

water and chloroform. Anal. Calcd for $C_{11}H_{12}N_2O_3$ (M = 220): C, 60.00; H, 5.45; N, 12.73. Found: C, 58.88; H, 5.47; N, 12.20. IR (KBr, selected bands, cm^{-1}): 3468 ν(OH), 3079 ν(NH), 1668 ν(C=O), 1632 ν(C=O···H), 1599 ν(C=N) and 750 ν(Ar). ^1H NMR (300.13 MHz, DMSO-d_6), δ: 2.41 (s, 3H, CH_3), 2.48 (s, 3H, CH_3), 6.91−7.67 (4H, Ar−H), 10.51 (s, 1H, OH), 14.58 (s, 1H, NH). $^{13}C\{^1H\}$ NMR (75.468 MHz, DMSO-d_6), δ: 26.5 (CH_3), 31.2 (CH_3), 114.9, 115.8, 120.2, and 126.2 (C_{Ar-H}), 129.3 ($C_{Ar\text{-}NH\text{-}N}$), 133.2 (C=N), 146.3 ($C_{Ar-OH}$), 196.2 and 196.4 (C=O).

Compound 2. Yield: 75% (based on 5,5-dimethylcyclohexane-1,3-dione), dark brown powder soluble in methanol, ethanol, acetone and insoluble in water and chloroform. Anal. Calcd for $C_{14}H_{16}N_2O_3$ (M = 260): C, 64.61; H, 6.15; N, 10.78. Found: C, 64.09; H, 6.38; N, 10.70. IR (KBr, selected bands, cm^{-1}): 3180 ν(OH), 2952 ν(NH), 1650 ν(C=O), 1616 ν(C=O···H), 1594 ν(C=N) and 759 ν(Ar). ^1H NMR (300.13 MHz, DMSO-d_6), δ: 1.02 (s, 6H, CH_3), 2.50 (s, 2H, CH_2), 2.57 (s, 2H, CH_2), 6.92−7.64 (3H, Ar−H), 10.75 (s, 1H, OH), 15.25 (s, 1H, NH). $^{13}C\{^1H\}$ NMR (75.468 MHz, DMSO-d_6), δ: 28.0 (CH_3), 30.4 (CH_3), 51.8 (CH_2), 51.8 (CH_2), 38.9 (C_{ipso}), 116.0, 120.3, 127.3, and 128.0 (C_{Ar-H}), 130.3 ($C_{Ar\text{-}NH\text{-}N}$), 137.0 (C=N), 147.2 ($C_{Ar-OH}$), 204.2 and 206.0 (C=O).

Compound 3. Yield: 83% (based on 5,5-dimethylcyclohexane-1,3-dione), dark brown powder soluble in methanol, ethanol, acetone and insoluble in water and chloroform. Anal. Calcd for $C_{14}H_{15}N_3O_5$ (M = 305): C, 55.08; H, 4.92; N, 13.77. Found: C, 55.00; H, 4.98; N, 13.68. IR (KBr, selected bands, cm^{-1}): 3448 ν(OH), 3100 ν(NH), 1665 ν(C=O), 1628 ν(C=O···H), 1596 ν(C=N) and 748 ν(Ar). ^1H NMR (400.13 MHz, DMSO-d_6), δ: 0.90−1.03 (s, 6H, CH_3), 2.50 (s, 2H, CH_2), 2.62 (s, 2H, CH_2), 7.22−7.74 (3H, Ar−H), 10.27 (s, 1H, OH), 14.91 (s, 1H, NH). $^{13}C\{^1H\}$ NMR (75.468 MHz, DMSO-d_6), δ: 28.0 (CH_3), 30.3 (CH_3), 52.0 (CH_2), 52.0 (CH_2), 38.7 (C_{ipso}), 110.7, 114.5, and 115.3 (C_{Ar-H}), 131.7 ($C_{Ar\text{-}NH\text{-}N}$), 136.1 (C=N), 144.8 ($C_{Ar\text{-}NO2}$), 149.0 ($C_{Ar-OH}$), 203.4 and 206.3 (C=O).

Compound 4. Yield: 61% (based on 1-ethoxybutane-1,3-dione), black powder soluble in methanol, ethanol, acetone and insoluble in water and chloroform. Anal. Calcd for $C_{12}H_{14}N_2O_4$ (M = 250): C, 57.60; H, 5.60; N, 11.20. Found: C, 57.75; H, 5.79; N, 11.07. IR (KBr, selected bands, cm^{-1}): 3238 ν(OH), 2963 ν(NH), 1661 ν(C=O), 1632 ν(C=O···H), 1601 ν(C=N) and 744 ν(Ar). ^1H NMR of a mixture of tautomeric enol-azo and hydrazone forms (300.13 MHz, DMSO-d_6). Enol-azo, δ: 1.03−1.07 (s, 3H, CH_3), 2.39 (s, 3H, CH_3), 4.21−4.25 (s, 2H, CH_2), 6.93−6.97 (4H, Ar−H), 10.41 (s, 1H, HO-Ar), 12.59 (s, 1H, HO-enol). Hydrazone, δ: 1.25−1.33 (s, 3H, CH_3), 2.39 (s, 3H, CH_3), 4.27−4.32 (s, 2H, CH_2), 7.00−7.56 (4H, Ar−H), 10.49 (s, 1H, Ar−OH), 14.68 (s, 1H, NH). $^{13}C\{^1H\}$ NMR (75.468 MHz, DMSO-d_6). Enol-azo, δ: 14.0 (CH_3), 26.6 (CH_3), 60.3 (CH_2), 114.3 (C−N), 114.8($C_{Ar-N=N}$), 120.1, 125.0, 126.0, 127.2, (C_{Ar-H}) 146.2, (C_{Ar-OH}), 165.2 (C=O), 193.2 (C−O). Hydrazone, δ: 14.2 (CH_3), 30.4 (CH_3), 60.8 (CH_2), 125.9, 115.6, 115.8 and 120.2, (C_{Ar-H}), 129.3 (C=N), 129.5 ($C_{Ar\text{-}NH\text{-}N}$), 145.7 ($C_{Ar-OH}$), 162.8 and 195.8 (C=O).

Compound 5. Yield: 69% (based on 1-ethoxybutane-1,3-dione), dark brown powder soluble in methanol, ethanol, acetone and insoluble in water and chloroform. Anal. Calcd for $C_{12}H_{13}N_3O_6$ (M = 295): C, 48.81; H, 4.41; N, 14.23. Found: C, 48.76; H, 4.41; N, 14.05. IR (KBr, selected bands, cm^{-1}): 3399 ν(OH), 3093 ν(NH), 1656 ν(C=O), 1632 ν(C=O···H), 1569 ν(C=N), 738 ν(Ar). ^1H NMR of a mixture of tautomeric enol-azo and hydrazone forms (300.13 MHz, DMSO-d_6). Enol-azo, δ: 1.27−1.34 (s, 3H, CH_3), 2.44−2.50 (s, 3H, CH_3), 4.27−4.29 (s, 2H, CH_2), 7.64−7.87 (3H, Ar−H), 11.44 (s, 1H, Ar−OH), 12.31 (s, 1H, HO-enol). Hydrazone, δ: 1.27−1.34 (s, 3H, CH_3), 2.50−2.51 (s, 3H, CH_3), 4.30−4.34 (s, 2H, CH_2), 7.64−7.87 (3H, Ar−H), 11.44 (s, 1H, Ar−OH), 14.25 (s, 1H, NH). $^{13}C\{^1H\}$ NMR (75.468 MHz, DMSO-d_6). Enol-azo, δ: 13.9 (CH_3), 26.6 (CH_3), 61.4 (CH_2), 110.0 (C−N), 110.2, ($C_{Ar-N=N}$), 114.0, 116.1 and 135.8, (C_{Ar-H}), 145.4 ($C_{Ar\text{-}NO2}$), 145.8 (C_{Ar-OH}), 163.8 (C=O) and 193.5 (C−O). Hydrazone, δ: 14.1 (CH_3), 30.6 (CH_3), 60.8 (CH_2), 113.5, 116.2, and 128.8 (C_{Ar-H}), 130.7, (C=N), 135.9 ($C_{Ar\text{-}NH\text{-}N}$), 142.9($C_{Ar\text{-}NO2}$), 143.6 ($C_{Ar-OH}$), 162.1 and 196.6 (C=O).

Preparation of Compound 6B. 0.01 mol of **6A** was dissolved in ethanol and 0.01 mol ethylenediamine was added and heated at 70 °C for 1 h. The precipitate was separated and recrystallized from methanol. Yield: 73% (based on **6A**), red powder soluble in methanol, ethanol, acetone and insoluble in chloroform. Anal. Calcd for $C_{13}H_{19}N_5O_5$ (M = 325.32): C, 48.00; H, 5.89; N, 21.53. Found: C, 48.04; H, 5.96; N, 20.97. IR (KBr, selected bands, cm^{-1}): 3346 ν(NH), 1672 ν(C=O), 1653 ν(C=O), 1636 ν(C=O), 1610 ν(C=N), 1508 ν(C−N) and 742 ν(Ar). ^1H NMR (300.13 MHz, DMSO-d_6). Enol-azo, δ: 2.23 (s, 3H, CH_3), 2.75 (s, 3H, CH_3), 3.44 (s, 2H, CH_2), 3.46 (s, 2H, CH_2), 7.09−7.68 (3H, Ar−H). Hydrazone, δ: 2.44 (s, 6H, CH_3), 3.44 (s, 2H, CH_2), 3.46 (s, 2H, CH_2), 7.09−7.68 (3H, Ar−H). $^{13}C\{^1H\}$ NMR (75.468 MHz, DMSO-d_6). Enol-azo, δ: 18.5 (CH_3), 31.3 (CH_3), 47.6 ($2CH_2$), 110.6 ($C_{Ar-N=N}$), 110.8 (C−N), 111.0, 113.7 and 134.5(C_{Ar-H}), 144.6 ($C_{Ar\text{-}NO2}$), 146.1 (C_{Ar-O}), 167.2 (C−O), 197.0 (C=O). Hydrazone, δ: 26.5 ($2CH_3$), 47.6 ($2CH_2$), 111.0, 113.7 and 134.5(C_{Ar-H}), 136.9 (C=N), 140.5 ($C_{Ar\text{-}NH\text{-}N}$), 144.6 ($C_{Ar\text{-}NO2}$), 146.1 ($C_{Ar-O}$), 196.4 (2C=O).

General Procedure for the Syntheses of the Copper(II) Complexes. To 90 mL of a 1.11×10^{-2} M acetone (**4**), methanol (**1**, **2**, **5**, **6B**) or ethanol (**3**) solution of **1**−**6B**, 10 mL of a 1×10^{-1} M aqueous solution of $Cu(NO_3)_2 \cdot 2.5H_2O$ were added under stirring, and the mixture was refluxed for 10 min and left for slow evaporation. The products (**7**−**12B**, correspondingly) usually started to precipitate in the reaction mixture after 2 days at room temperature; after 4 days they were filtered off, washed with a small amount of ethanol, and dried in air. Specific details for each compound are given below.

Compound 7. Yield 50% (based on Cu). Black powder soluble in acetone, methanol, ethanol, acetonitrile, and DMSO. Anal. Calcd for $C_{24}H_{28}N_4O_8Cu_2$ (M = 627.6): C, 45.93; H, 4.50; N, 8.93. Found: C, 46.08; H, 4.50; N, 9.16. MS (ESI): m/z: 656 $[M+H]^+$. IR (KBr, selected bands, cm^{-1}): 1639 ν(C=O), 1631 ν(C=O), 1584 ν(C=N), 755 ν(Ar). UV−vis (pH 4.5): λ_{max} = 428 nm, $\Delta\lambda$ = 45 nm, ε = 10900 L mol^{-1} cm^{-1}.[8b]

Compound 8. Yield 73% (based on Cu). Dark brown powder soluble in acetone, methanol, ethanol, acetonitrile, and DMSO. Anal. Calcd for $C_{28}H_{32}N_4O_8Cu_2$ (M = 679.7): C, 49.48; H, 4.75; N, 8.24. Found: C, 50.06; H, 4.66; N, 8.46. MS (ESI): m/z: 666 $[M+H]^+$. IR (KBr, selected bands, cm^{-1}): 1655 ν(C=O), 1619 ν(C=O), 1588 ν(C=N), 758 ν(Ar). UV−vis (pH 5): λ_{max} = 449 nm, $\Delta\lambda$ = 76 nm, ε = 9750 L mol^{-1} cm^{-1}.

Compound 9. Yield 71% (based on Cu). Dark brown powder soluble in acetone, methanol, ethanol, acetonitrile, and DMSO. Anal. Calcd for $C_{14}H_{15}N_3O_6Cu$ (M = 384.8): C, 43.69; H, 3.93; N, 10.92. Found: C, 43.87; H, 3.84; N, 10.62. MS (ESI): m/z: 757 $[M+H]^+$. IR (KBr, selected bands, cm^{-1}): 1647 ν(C=O), 1604 ν(C=N), 746 ν(Ar). UV−vis (pH 4): λ_{max} = 457 nm, $\Delta\lambda$ = 43 nm, ε = 17300 L mol^{-1} cm^{-1}.

Compound 10. Yield 47% (based on Cu). Greenish black powder soluble in acetone, methanol, ethanol, acetonitrile, and DMSO. Anal. Calcd for $C_{24}H_{24}N_4O_8Cu_2$ (M = 623.6): C, 46.23; H, 3.88; N, 8.98. Found: C 46.71; H 3.94; N 9.06. MS (ESI): m/z: 369 $[M+H]^+$. IR (KBr, selected bands, cm^{-1}): 1668 ν(C=O), 1611 ν(C=O), 1599 ν(C=N), 755 ν(Ar). UV−vis (pH 5): λ_{max} = 404 nm, $\Delta\lambda$ = 149 nm, ε = 9000 L mol^{-1} cm^{-1}.

Compound 11. Yield 58% (based on Cu). Dark brown powder soluble in acetone, methanol, ethanol, acetonitrile, and DMSO. Anal. Calcd for $C_{12}H_{13}N_3O_7Cu$ (M = 374.8); C, 38.46; H, 3.50; N, 11.21. Found: C, 38.97; H, 3.56; N, 11.49. MS (ESI): m/z: 409 $[M+H]^+$. IR (KBr, selected bands, cm^{-1}): 1686 ν(C=O), 1638 ν(C=O), 1604 ν(C=N), 747 ν(Ar). UV−vis (pH 3.5): λ_{max} = 424 nm, $\Delta\lambda$ = 41 nm, ε = 15500 L mol^{-1} cm^{-1}.

Synthesis of complexes 12A and 12B and their interconversion. Compound 12A. The preparation of the complex **12A** from **6A** is

similar to the synthesis of the compounds **7**−**11** described above and reported by us before.[4a] Thus, to 90 mL of 1.11×10^{-2} M ethanol solution of H_2L^6, 10 mL of 1×10^{-1} M aqueous solution of $Cu(NO_3)_2 \cdot 2.5H_2O$ and 5−6 drops of 0.01 M HCl (to reach pH 2) were added. The mixture was stirred under solvent reflux for 10 min and left for slow evaporation. Greenish-black crystals started to form in the reaction mixture after 2 d at room temperature; after 4 d they were filtered off and dried in air. Yield 70% (based on Cu). Anal. Calcd for $C_{22}H_{22}Cu_2N_6O_{12}$ (M = 689.54): C 38.32, H 3.22, N 12.19. Found: C 38.32, H 3.14, N 11.98. IR (KBr, selected bands, cm^{-1}): 3468 ν(OH), 1652 ν(C=O), 1611 ν(C=O···H), 1602 ν(C=N), 745 ν(Ar).

Compound 12B. A methanol/water (5/1, v/v) solution (50 mL) of **6B** (0.01 mol) was added to 0.01 mol copper(II) nitrate hydrate, and the mixture was stirred under reflux for 5 min and then left for slow evaporation. Yield 50% (based on Cu). Greenish black powder soluble in acetone, methanol, ethanol, acetonitrile, and DMSO. Anal. Calcd for $C_{11}H_{13}N_3O_7Cu$ (M = 362.8): C, 36.42; H, 3.61; N, 11.58. Found: C, 36.75; H, 3.62; N, 11.76. IR (KBr, selected bands, cm^{-1}): 1673 and 1636 ν(C=O), 1599 ν(C=N), 746 ν(Ar). UV−vis (pH 5): λ_{max} = 439 nm, $\Delta\lambda$ = 47 nm, ε = 19200 L mol^{-1} cm^{-1}.

Conversion of 12B to 12A. A methanol solution (10 mL) of **12B** (0.01 mol) was refluxed for 8 h, whereafter it was left at room temperature for slow evaporation. After about 2 d, crystals of **12A** started to form, and their identity was confirmed by elemental analysis and also by comparison of IR data and the X-ray unit cell with those of the genuine compound.

Syntheses of the Schiff-Base Cu Complexes. Compound 13. To an aqueous-ethanol (20/80, v/v, 50 mL) solution of **6** (10 mmol) were added $Cu(NO_3)_2 \cdot 2.5H_2O$ (10 mmol), ethylenediamine (10 mmol), and 5 mL of 0.01 M HCl (pH 2); then the mixture was refluxed for 5 min and left for slow evaporation. The crystals of **13** started to form in the reaction mixture after about 2 d at room temperature. The product was filtered off, washed with a small amount of water, and dried in air. Yield 34% (based on Cu). Greenish black powder soluble in acetone, methanol, ethanol, acetonitrile, and DMSO. Anal. Calcd for $C_{13}H_{15}N_5O_4Cu$ (M = 368.8): C, 42.33; H, 4.10; N, 18.99. Found: C, 42.45; H, 4.03; N, 18.63. IR (KBr, selected bands, cm^{-1}): 1646 ν(C=O), 1601 ν(C=N), 1560 ν(C=N), 749 ν(Ar).

Synthesis of 14 from 12B. An ethanol−water (1:1, v/v, 50 mL) solution with 0.01 mol of **12B**, en (0.01 mol), and 1 mL of 0.01 M HCl (pH 2) was refluxed for 5 min and then evaporated at room temperature; after about 3 d, crystals of **14** started to form. Yield 37% (based on Cu). Dark brown crystals soluble in acetone, methanol, ethanol, acetonitrile, and DMSO. Anal. Calcd for $C_{13}H_{15}N_5O_4Cu$ (M = 368.8): C, 42.33; H, 4.10; N, 18.99. Found: C, 41.16; H, 4.22; N, 18.55. IR (KBr, selected bands, cm^{-1}): 1634 ν(C=O), 1588 ν(C=N), 1546 ν(C=N), 748 ν(Ar).

Conversion of 12A to 14. An ethanol solution (50 mL) with 0.01 mol of **12A** and en (0.01 mol) was refluxed for 8 h, and then was left for evaporation at room temperature; after about 2 d, crystals of **14** started to form; their identity was confirmed by elemental analysis, also by comparison of IR spectra and the X-ray unit cell with those of the genuine compound.

Computation Details. The full geometry optimization of all structures was carried out at the DFT/HF hybrid level of theory using the Becke's three-parameter hybrid exchange functional in combination with the gradient-corrected correlation functional of Lee, Yang, and Parr (B3LYP)[22] with the help of the Gaussian-98 program package.[23] The restricted approximations for the structures with closed electron shells and the unrestricted methods for the structures with open electron shells were employed. Symmetry operations were not applied for all structures. The geometry optimization was carried out using a relativistic Stuttgart pseudopotential that described 10 core electrons and the appropriate contracted basis sets (8s7p6d)/[6s5p3d][24] for the copper atoms and the 6-31G(d) basis sets for other atoms. The Hessian matrix was calculated analytically for structures to prove the location of correct minima (no imaginary frequencies) and to estimate the thermodynamic parameters, the latter being calculated at 25 °C. Solvent effects (δE_s) were taken into account at the single-point calculations on the basis of the gas-phase geometries at the CPCM-B3LYP/6-31+G(d)//gas-B3LYP/6-31G(d) level of theory using the polarizable continuum model[25] in the CPCM version[26] with DMSO and water taken as solvents. The enthalpies and Gibbs free energies in solution (H_s and G_s) were estimated by addition of the solvent effect δE_s to the gas-phase values H_g and G_g. Several possible conformations for each structure were calculated and only the most stable ones are discussed.

X-ray Structure Determinations. X-ray quality single crystals of ligands (**4** and **5**) and complexes were grown by slow evaporation at room temperature of methanol (**7**), water−methanol (**8**, **12**), water−ethanol (**9**, **11**, **13**), or water-acetone (**10**) solutions. They were immersed in cryo-oil, mounted in a Nylon loop, and measured at a temperature of 150 K (also 299 K for **4** and **5**). Intensity data were collected using a Bruker AXS-KAPPA APEX II diffractometer with graphite monochromatic Mo−Kα (λ 0.71073) radiation. Data were collected using ω scans of 0.5° per frame and full sphere of data were obtained. Cell parameters were retrieved using Bruker SMART software and refined using Bruker SAINT[27] on all the observed reflections. Absorption corrections were applied using SADABS.[28] Structures were solved by direct methods by using the SHELXS−97 package[28] and refined with SHELXL−97.[29a] Calculations were performed using the WinGX System−Version 1.80.03.[29b] All hydrogens were inserted in calculated positions. Least square refinements with anisotropic thermal motion parameters for all the non-hydrogen atoms and isotropic for most of the remaining atoms (some exceptions in the structures of **10**, **11**, and **12** because of a poorer quality of crystals) were employed. Crystallographic and selected structural details are listed in Supporting Information, Tables S1 and S2 respectively. CCDC 784258−784269 contain the supplementary crystallographic data for this paper. These data can be obtained free of charge from The Cambridge Crystallographic Data Centre via www.ccdc.cam.ac.uk/data_request/cif.

Catalytic Studies. Oxidation of Cyclohexane. The reaction mixtures were prepared as follows: to 1−10.0 μmol of the complex **7**−**13** contained in the reaction flask were added 4 mL of MeCN, 0.01−0.1 mmol HNO_3, 1−5.0 mmol C_6H_{12}, and 10.0 mmol H_2O_2 (30% in H_2O), in this order. The reaction mixture was stirred for 6 h at room temperature (ca. 25 °C) and air atmospheric pressure, then 90 μL of cycloheptanone (as internal standard) and 9.0 mL of diethyl ether (to extract the substrate

(22) (a) Becke, A. D. *J. Chem. Phys.* **1993**, *98*, 5648. (b) Lee, C.; Yang, W.; Parr, R. G. *Phys. Rev.* **1988**, *B37*, 785.
(23) Frisch, M. J.; Trucks, G. W.; Schlegel, H. B.; Scuseria, G. E.; Robb, M. A.; Cheeseman, J. R.; Zakrzewski, V. G.; Montgomery, J. A.; Stratmann, Jr., R. E.; Burant, J. C.; Dapprich, S.; Millam, J. M.; Daniels, A. D.; Kudin, K. N.; Strain, M. C.; Farkas, O.; Tomasi, J.; Barone, V.; Cossi, M.; Cammi, R.; Mennucci, B.; Pomelli, C.; Adamo, C.; Clifford, S.; Ochterski, J.; Peterson, G. A.; Ayala, P. Y.; Cui, Q.; Morokuma, K.; Malick, D. K.; Rabuck, A. D.; Raghavachari, K.; Foresman, J. B.; Cioslowski, J.; Ortiz, J. V.; Baboul, A. G.; Stefanov, B. B.; Liu, G.; Liashenko, A.; Piskorz, P.; Komaromi, I.; Gomperts, R.; Martin, R. L.; Fox, D. J.; Keith, T.; Al-Laham, M. A.; Peng, C. Y.; Nanayakkara, A.; Challacombe, M.; Gill, P. M. W.; Johnson, B.; Chen, W.; Wong, M. W.; Andres, J. L.; Gonzalez, C.; Head-Gordon, M.; Replogle, E. S.; Pople, J. A. *Gaussian 98*, revision A.9; Gaussian, Inc.: Pittsburgh, PA, 1998.
(24) Dolg, M.; Wedig, U.; Stoll, H.; Preuss, H. *J. Chem. Phys.* **1987**, *86*, 866.
(25) Tomasi, J.; Persico, M. *Chem. Rev.* **1997**, *94*, 2027.
(26) Barone, V.; Cossi, M. *J. Phys. Chem.* **1998**, *102*, 1995.
(27) *APEX2 & SAINT*; Bruker AXS Inc.: Madison, WI, 2004.
(28) Sheldrick, G. M. *Acta Crystallogr., Sect. A* **1990**, *46*, 467.
(29) (a) Sheldrick, G. M. *Acta Crystallogr., Sect. A* **2008**, *64*, 112. (b) Farrugia, L. J. *J. Appl. Crystallogr.* **1999**, *32*, 837.

and the products from the reaction mixture) were added. The resulting mixture was stirred for 15 min, and then a sample taken from the organic phase was analyzed by GC. The GC analyses of the aqueous phase showed the presence of only traces (less than 0.05%) of oxidation products. Blank experiments were performed and confirmed that no cyclohexane oxidation products (or only traces, below 0.3%) were obtained in the absence of the metal catalyst. The formation of CyOOH was proved by using Shul'pin's method[17,18] based on the effect of addition of PPh_3 (prior to GC analysis) on the amounts of cyclohexanol and cyclohexanone (PPh_3 converts CyOOH into CyOH). For the experiments performed in a sealed tube, the following reaction procedure was used: to 10.0 μmol of complex **7** contained in the Pyrex tube were added 0.5−1 mL of MeCN, 0.1 mmol HNO_3, 1 mmol C_6H_{12}, and 2.0 mmol H_2O_2 (30% in H_2O), in this order. The tube was closed and placed in the focused microwave reactor (or oil bath). The system was left under stirring and irradiation for 1 h at 50 °C. After the reaction mixture was cooled down, 3.5−3 mL of MeCN, 90 μL of cycloheptanone (as internal standard), and 9.0 mL of diethyl ether (to extract the substrate and the products from the reaction mixture) were added. The resulting mixture was stirred for 15 min, and then a sample taken from the organic phase was analyzed by GC.

Aerobic Oxidation of Alcohols in Aqueous Solutions. The reactions were carried out according to the procedure described earlier.[4a,19] They were performed in flasks fitted with water circulating condensers under atmospheric pressure of air. All reagents were placed into the flask, and the resulting mixture was then heated with continuous stirring in an oil bath. The reaction mixtures after the oxidation reaction were neutralized by 1 M HCl, and then 10 mL of EtOAc was added for the extraction. The organic phase was analyzed by gas chromatography using acetophenone as the internal standard.

Microwave-Assisted Oxidation of Alcohols with TBHP. To 0.01 mmol of the catalyst contained in a Pyrex tube were added 5 mmol of the alcohol substrate [i.e., benzyl alcohol or 1-phenylethanol] and 10 mmol of TBHP. The tube was closed and placed in the focused microwave reactor. The system was left under stirring and irradiation for 15−240 min at 50 °C (in case of benzyl alcohol) or 80 °C (in case of 1-phenylethanol). The power of 10 W was selected for all experiments. After the reaction, the mixture was allowed to cool down, 5 mL of MeCN and internal standard (i.e., 75 μL of acetophenone in the case of benzyl alcohol oxidation and 300 μL of benzaldehyde in the case of 1-phenylethanol oxidation) were added. Small aliquots (about 50 μL) were then taken, diluted 10 times by MeCN, and subjected to the GC analysis.

Acknowledgment. This work has been partially supported by the Foundation for Science and Technology (FCT), Portugal, and its PPCDT (FEDER funded). K.T.M., P.J.F., and Y.Y.K. express gratitude to the FCT for their postdoc and doctoral fellowships. M.N.K., MLK, and K.V.L. are grateful to the FCT and IST for research contracts within the Ciência 2007 and Ciência 2008 scientific programs. The authors thank the Portuguese NMR Network (IST-UTL Centre) for providing access to the NMR facility.

Supporting Information Available: Tables listing crystallographic data, atomic coordinates, bond lengths and bond angles, anisotropic displacement parameters, hydrogen coordinates and isotropic displacement parameters, torsion angles and hydrogen bonds, calculated total energies, enthalpies and Gibbs free energies. X-ray crystallographic data for **4**, **7**−**14** in CIF format. Packing diagram of **4**, **7**−**14**. This material is available free of charge via the Internet at http://pubs.acs.org.